Article

Current Biology

A salivary factor binds a cuticular protein and modulates biting by inducing morphological changes in the mosquito labrum

Graphical abstract

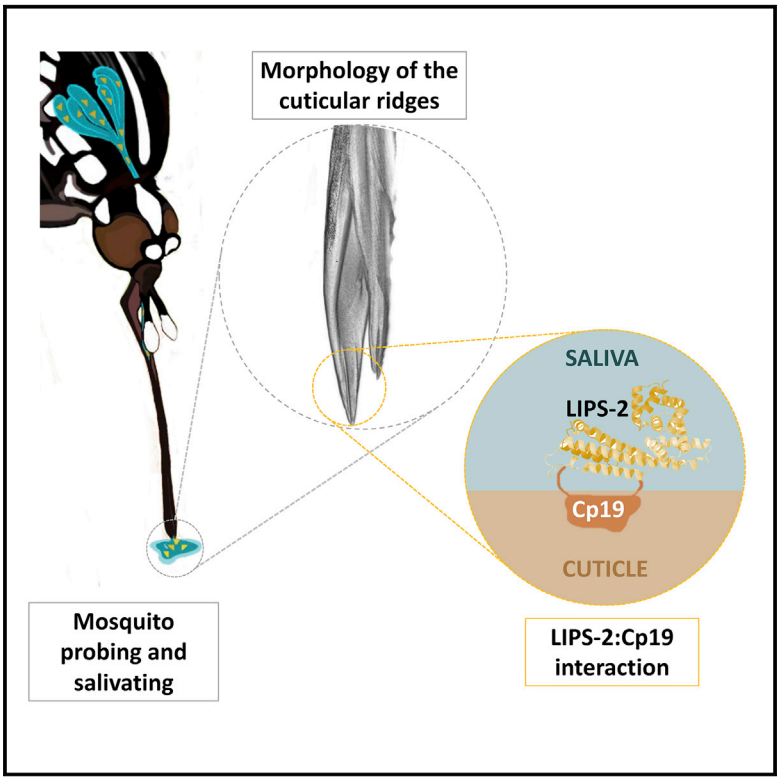

Highlights

- LIPS-2 in the mosquito saliva controls intradermal probing before engorging blood
- LIPS-2 binds Cp19, a cuticular protein found at the tip of the labrum
- Binding of LIPS-2 causes a morphological change of the structures of the labrum
- LIPS-2 structural characterization provides insights into its interaction with Cp19

Authors

Irene Arnoldi, Giulia Mancini, Marco Fumagalli, ..., Paolo Iadarola, Federico Forneris, Paolo Gabrieli

Correspondence

federico.forneris@unipv.it (F.F.), paolo.gabrieli@unimi.it (P.G.)

In brief

Arnoldi et al. describe a novel role of the mosquito saliva, a feedback signaling pathway affecting intradermal probing preceding blood feeding. The initial trigger of this signaling pathway in *Aedes* mosquitoes is the interaction between LIPS-2, a salivary protein, and Cp19, a cuticular protein found at the tip of the mosquito mouth.

Arnoldi et al., 2022, Current Biology *32*, 1–12
August 22, 2022
https://doi.org/10.1016/j.cub.2022.06.049

CellPress

Current Biology

CellPress
OPEN ACCESS

Article

A salivary factor binds a cuticular protein and modulates biting by inducing morphological changes in the mosquito labrum

Irene Arnoldi,[1,2,3,6] Giulia Mancini,[1,6] Marco Fumagalli,[1,4] Dario Gastaldi,[5] Luca D'Andrea,[5] Claudio Bandi,[2,3] Monica Di Venere,[4] Paolo Iadarola,[4] Federico Forneris,[1,7,*] and Paolo Gabrieli[1,2,3,8,9,*]

[1]The Armenise-Harvard Laboratory of Structural Biology, Department Biology and Biotechnology, University of Pavia, via Ferrata 9, 27100 Pavia, Italy
[2]Entopar lab, Department of Biosciences, University of Milan, via Celoria 26, 20133, Milan, Italy
[3]Centro Interuniversitario di Ricerca sulla Malaria/Italian Malaria Network, Milan, Italy
[4]Biochemistry Unit, Department Biology and Biotechnology, University of Pavia, Via Taramelli 3, 27100 Pavia, Italy
[5]Laboratory of Biological Structure Mechanics (LaBS), Department of Chemistry, Materials and Chemical Engineering Giulio Natta, Politecnico di Milano, Piazza Leonardo da Vinci 32, 20133, Milano, Italy
[6]These authors contributed equally
[7]Twitter: @fornerislab
[8]Twitter: @gab_paolo
[9]Lead contact
*Correspondence: federico.forneris@unipv.it (F.F.), paolo.gabrieli@unimi.it (P.G.)
https://doi.org/10.1016/j.cub.2022.06.049

SUMMARY

The mosquito proboscis is an efficient microelectromechanical system, which allows the insect to feed on vertebrate blood quickly and painlessly. Its efficiency is further enhanced by the insect saliva, although through unclear mechanisms. Here, we describe the initial trigger of an unprecedented feedback signaling pathway in *Aedes* mosquitoes affecting feeding behavior. We identified LIPS proteins in the saliva of *Aedes* mosquitoes that promote feeding in the vertebrate skin. LIPS show a new all-helical protein fold constituted by two domains. The N-terminal domain interacts with a cuticular protein (Cp19) located at the tip of the mosquito labrum. Upon interaction, the morphology of the labral cuticle changes, and this modification is most likely sensed by proprioceptive neurons. Our study identifies an additional role of mosquito saliva and underlines that the external cuticle is a possible site of key molecular interactions affecting the insect biology and its vector competence.

INTRODUCTION

Mosquitoes transmit a large number of different pathogens to humans, including protists, nematodes, and viruses, which can cause debilitating, sometimes untreatable and potentially deadly diseases with devasting socio-economic impacts.[1] Every year mosquito-borne diseases collectively account for more than 17% of all infections worldwide, and they are estimated to cause more than 700,000 deaths annually, with most of the human population living in countries at risk of contracting these diseases.[2] The high vectorial capacity of mosquitoes largely resides in their reproductive strategy: females need a vertebrate host to complete oogenesis, and each individual performs multiple reproductive cycles in her lifetime. When a female mosquito takes blood from an infected human host, most pathogens pass in the mosquito midgut and replicates inside the insect body, eventually reaching the salivary glands. During subsequent bites, mosquitoes transfer the pathogens to new hosts injecting them together with the saliva.[3] Complex interactions between three organisms occur at the bite site: the vertebrate host, which mounts its immune response against the pathogen and the mosquito saliva;[4] the mosquito vector, which tries to reach a blood vessel in a short time to acquire the blood;[5] and the pathogen, which tries to establish the infection.[6] Understanding the biological pathways and interactions that occur in this microenvironment is fundamental to prevent mosquito biting and pathogen spread, an important goal in global public health interventions.

The success of pathogen infection, of the mosquito biting and of the human immune response largely depends on the mosquito saliva, a cocktail of pharmacologically relevant proteins, whose identity and molecular function vary among the mosquito species.[7] Salivary proteins are immunogens and allergens, they have vasodilatory and anticlotting activities that facilitate blood feeding, and they exert a complex action on the human immune system, which result in the enhancement of the infection of co-inoculated viruses and pathogens.[8–14] Contrasting evidence has been reported to support the function of the mosquito saliva during blood feeding. Mosquitoes completely lacking the salivary glands can take the same amount of blood as those having saliva, but they are slower in trespassing the skin barrier,[5,15,16] even if a later study suggests that females not able to salivate

Please cite this article in press as: Arnoldi et al., A salivary factor binds a cuticular protein and modulates biting by inducing morphological changes in the mosquito labrum, Current Biology (2022), https://doi.org/10.1016/j.cub.2022.06.049

have defects also in acquiring a blood meal.[17] Anyhow, these data firmly indicate that one of the effects of the saliva is to decrease the time that the mosquitoes take to pierce the skin surface and to insert the stylet to look for blood, a process defined as "intradermal probing."[18,19] Despite this evidence, little is known about the mechanisms that regulate the initial phases of mosquito feeding and the factors associated with the saliva that are required during this process. It has been proposed that spotting a blood vessel might be facilitated by the salivary anticlotting and immunomodulatory activities because of an indirect effect.[20] For example, the apyrase hydrolyzes ATP and ADP, which induce vasoconstriction and mediate the activation and aggregation of platelets, avoiding coagulation and facilitating blood vessel location and blood engorgement.[21] A similar effect has been described for other factors, such as the anopheline antiplatelet protein.[22] On the other side, the allergic response to the saliva allergens can stimulate degranulation of the mast cells residing in the skin of the vertebrate host, inducing in turn vasodilation.[23]

Considering the central role of mosquito saliva in quicken blood feeding, we looked for factors that can regulate this biological trait through a direct effect. We focused our attention on the salivary proteins of *Aedes albopictus* female mosquitoes, a highly invasive pest species and emerging vectors of many arboviruses in temperate regions.[24,25]

In this study, we show that saliva components can establish a feedback mechanism in *Aedes* mosquitoes through protein-protein interactions occurring at the tip of the labrum. We demonstrate that a salivary protein secreted during the initial phases of the biting process, which we named labrum-interacting protein of the saliva 2 (LIPS-2), directly interacts with a cuticular protein at the tip of the labrum (Cp19). We found that the LIPS-2:Cp19 interaction induces a change in the morphology of the cuticle and affects mosquito intradermal probing before blood engorgement. These findings point at the multifunctional role of mosquito saliva and of the mouth's cuticle, which is not merely an external exoskeleton forming strong structures, allowing the insect, for example, to feed or sting, but it is also a site of key molecular interactions governing the animal biology. Furthermore, our study deepens the knowledge of the feeding mechanism in mosquitoes, opening new ways to target and alter the mosquito feeding process.

RESULTS

LIPS are prominent factors in the *Aedes* female saliva

Since *Ae. albopictus* salivary proteins were previously identified using transcriptomic analysis of the salivary gland extracts,[26] our first aim was the identification of bona fide proteins that are transferred during feeding to a vertebrate host in the mosquito saliva.

To explore the content of the *Ae. albopictus* saliva, we have analyzed the saliva forcedly expectorated by mature females using the cholinomimetic drug Pilocarpine[27] (Table S1; Figure 1A). Wondering which of the identified proteins might be strictly related to blood feeding, considering that female mosquitoes feed also on floral nectars,[28–30] we compared the salivary glands secretome from young (1-day-old) and mature (6-day-old) mosquitoes using 2D gel analyses (Figures 1B and S1; distance-based ANOVA of fuzzy maps: pseudo-F = 1.73, $p < 0.05$; 999 permutations). *Aedes* mosquitoes, indeed, usually take blood only few days after emergence:[31] we expected that the amount of proteins linked to blood feeding would have increased during sexual maturation, as already noted in the case of SGS proteins in *Aedes aegypti*.[32] Notably, we also found that protein quantities decreased soon after blood meal, as visible in 2D gel analyses (Figure 1A; pseudo-F = 2.19, $p < 0.01$; 999 permutations) in accordance to previous findings.[29]

To further increment our confidence in identifying proteins essential for blood feeding, we searched for common factors also in the expectorated saliva of the yellow fever mosquito *Ae. aegypti*.[33,34] We shortlisted the candidate molecules based on their expression in the female salivary glands[26] and based on their proved immunogenicity in humans.[35,36] Aiming at proteins possibly affecting biting in females, we excluded those targets with known or confidently predicted functions related to blood clotting and/or immunity. The summary of these analyses is shown in Figure 1F.

We therefore focused our attention on a class of orphan proteins known as 34k- based on their apparent molecular weight of 34 kDa. *34k-* ortholog genes have been found exclusively in members of the Culicinae subfamily, not in the Anophelinae clade. Their intron-less genes suggest a relatively recent horizontal transfer from prokaryotic organisms or viruses or a *de novo* origin occurred in this specific class of organisms. In *Ae. aegypti*, the *34k-2* gene is duplicated on the same chromosome (VectorBase: AAEL003601 and AAEL7872), whereas the *34k-1* is a single-copy gene (VectorBase: AAEL3600). In *Ae. albopictus*, two 34k-gene clusters have been assembled (VectorBase: AALF017483-AALF017486 and AALF004419-AALF004424): in both the clusters, one *34k-2* like gene is present (VectorBase: AALF017486 and AALF004419), whereas the other genes, except for AALF004420, are closely similar to *34k-1*. Nevertheless, sequencing[26] and our proteomic analyses have revealed the expression of two main genes in the salivary glands, closely similar to AALF017486 and AALF017483. We named these genes and their associated products *labrum-interacting protein of the saliva-1 and -2* (*LIPS-1* and *LIPS-2*), based on the results reported in this report, and hereafter, they will be named accordingly. The *LIPS-2* gene product from both species is immunogen in humans[37] and shifts the vertebrate immune response toward a Th2 phenotype,[9,11,33] enhancing the viremia *in vitro* and *in vivo* of a number of arboviruses transmitted by mosquitoes. Furthermore, *LIPS-2* expression is enhanced in the salivary glands during dengue infection and enhances dengue virus replication in human keratinocytes.[11,38] We first assessed whether these proteins are involved in biting and blood feeding processes using an *in vivo* functional analysis through RNA interference.

The presence of LIPS proteins in *Aedes* saliva is critical for biting

LIPS-1/*LIPS-2* knockdown (KD) females, generated by injecting *in vitro* synthesized dsRNA in the thorax of 1-day-old mosquitoes, showed strongly increased feeding time (Figures 2 and S2), with marked enhanced time spent on the skin looking for blood (i.e., intradermal probing).[39] Whenever the mosquitoes eventually started feeding, *LIPS* KD females took the same amount of time to engorge blood (Figure 2).

Please cite this article in press as: Arnoldi et al., A salivary factor binds a cuticular protein and modulates biting by inducing morphological changes in the mosquito labrum, Current Biology (2022), https://doi.org/10.1016/j.cub.2022.06.049

CellPress
OPEN ACCESS

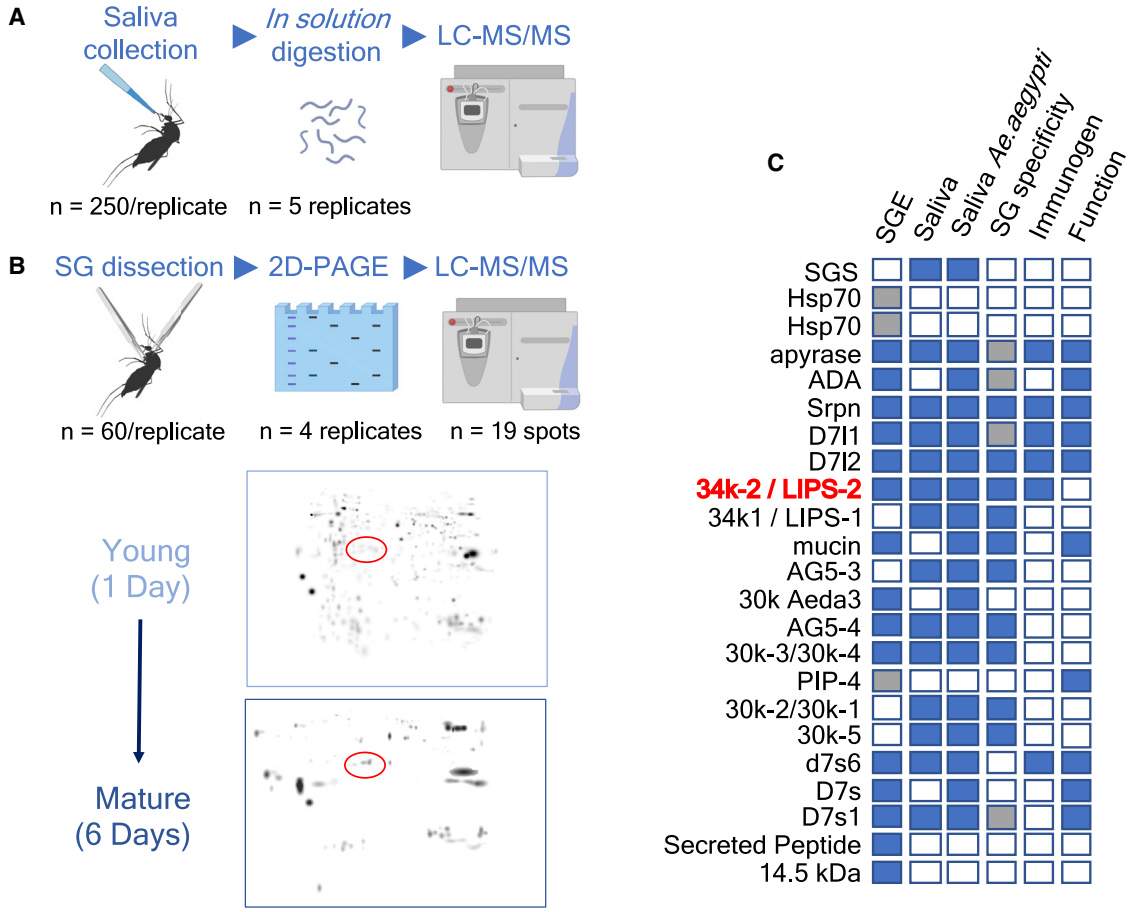

Figure 1. Identification of proteins in the *Ae. albopictus* saliva

(A) Schematic representation of the employed saliva extraction protocol and the LC-MS/MS *in solution* analysis of the recovered proteins. Schemes were created using BioRender.com.

(B) Schematic representation of the protocol used for the analysis of the salivary gland homogenates and the identification of the 2D-gel spots. The master gels obtained by combining four different replicates are shown for salivary glands dissected from young (1-day-old) and sexually mature (6-day-old) *Ae. albopictus* females. A red circle helps the localization of the LIPS-2 spots in the gel map. Schemes were created as in (A).

(C) List of the identified proteins in either saliva or salivary glands homogenates derived from the LC-MS/MS analysis coupled with the available information from literature. The boxes are blue when the protein has been identified either in the extracts (SGE) and/or in the expectorated saliva, if homologous proteins have been reported in the *Aedes aegypti* saliva, if the expression of its gene is restricted to the female salivary glands at adult stage, if the protein has been previously recognized as immunogen and/or as a possible allergen and if the function of the protein has been characterized or suggested. In the case of SGE analysis, some of the proteins have been identified in the SGE from 1-day-old females, and the boxes are colored in gray. Gray boxes have been also used in the column showing the tissue-specific expression because some of the genes (such as apyrase) are heavily overexpressed in the female salivary glands, but their expression is not exactly restricted to this tissue. Vice versa, the boxes are white.

See also Table S1 and Figure S1.

Considering that previous reports showed LIPS-2 and not LIPS-1 as a key salivary antigen[36] and the lower *LIPS-1* expression levels,[26] we wondered whether LIPS-2 might display a more prominent role than LIPS-1 in affecting this behavior. To test this hypothesis, we generated *LIPS-2* KD females and verified that the effect of gene silencing on the time spent by mosquitoes in intradermal probing was as strong as in *LIPS-1/LIPS-2* double-KD females (Figure 2; Video S1). In addition, in this case, females that were able to complete a blood meal engorged the same amount of blood as control females (Figure S2).

These results demonstrated that LIPS-2 is a factor affecting the initial phases of mosquito biting and prompted us to assess if LIPS-2 can affect biting with a direct effect on the mosquito proboscis.

Recombinant LIPS-2 interacts with the mosquito labrum end tip and is sufficient to trigger salivation and probing

Purified recombinant *Ae. albopictus* LIPS-2 (albLIPS-2) applied to the stylet fascicle of adult mosquito females after removal of the labium yielded unexpected reactions. *Ae. albopictus* mosquitoes exposed to albLIPS-2 reacted by moving the mouth apparatus, particularly oscillating the maxillae and the labrum (Figure 3A; Video S2). These movements, not observed in mosquitoes exposed to control proteins (e.g., BSA), are characteristic of what can be normally observed *in vivo* during the

Please cite this article in press as: Arnoldi et al., A salivary factor binds a cuticular protein and modulates biting by inducing morphological changes in the mosquito labrum, Current Biology (2022), https://doi.org/10.1016/j.cub.2022.06.049

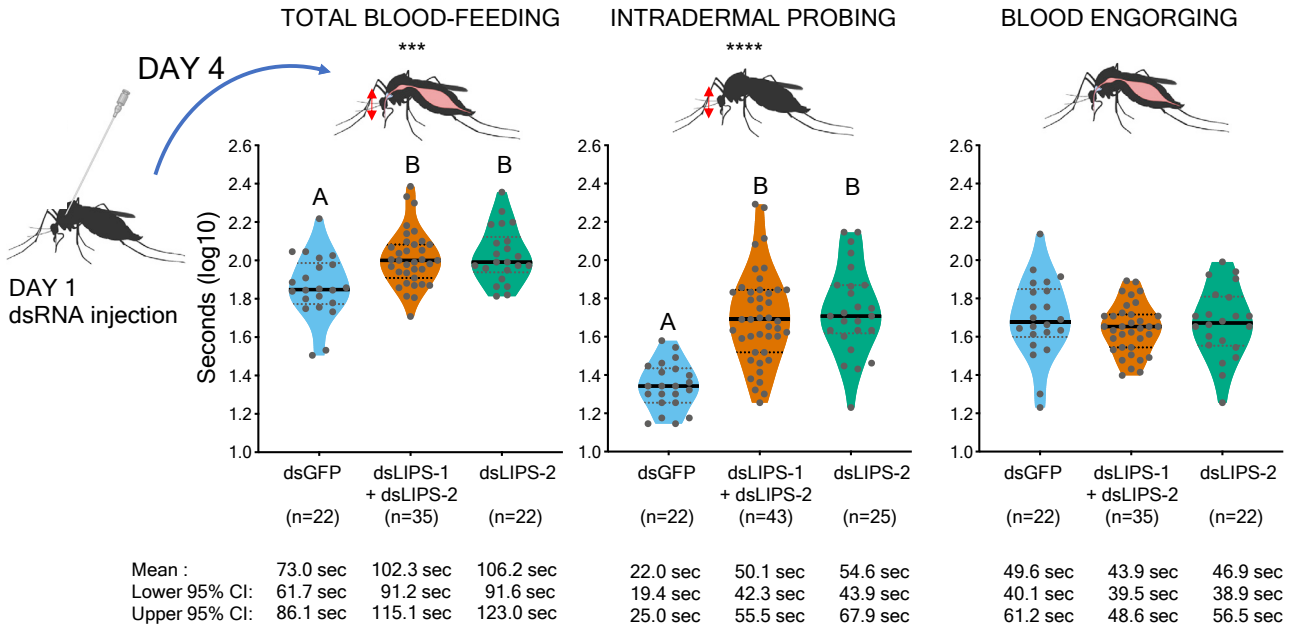

Figure 2. Knockdown of LIPS expression impairs the length of intradermal probing prior blood engorgement

Ae. albopictus females have been injected with dsRNA-matching *GFP* as control (*dsGFP*, light blue) or *LIPS-1* and *LIPS-2* (*dsLIPS-1* + *dsLIPS-2*, orange; *dsLIPS-2*, green) soon after emergence from pupal case. After 3 days (on day 4), the ability of females to feed has been tested by measuring the time spent in feeding (left). Before applying a statistical analysis for hypothesis testing, the data have been $\log_{10}$-transformed because raw data were not normally distributed, and the new log-transformed data have been used for subsequent analysis and presented in the graph. Females injected with *dsLIPS* showed increased feeding time ($F(2, 76) = 8.297$; $p = 0.0006$; Tukey's multiple comparison: *dsLIPS1* + *dsLIPS2* versus *dsGFP*, $p = 0.0016$; *dsLIPS2* versus *dsGFP*, $p = 0.0017$). *dsLIPS*-injected females spent longer time searching under the skin for a blood vessel (center) (Welch's ANOVA $W(2,53) = 45.59$, $p < 0.0001$; Dunnett's T3 multiple comparison: dsLIPS1+dsLIPS2 versus dsGFP, $p < 0.0001$; dsLIPS2 versus dsGFP, $p < 0.0001$). The time spent engorging blood was similar for mosquitoes treated with *dsGFP* or *dsLIPS* (right) ($F(2,76) = 0.6828$, $p = 0.5083$). The number of females (n) is shown for each pool: some of the females from *dsLIPS*-injected groups did probe, but they were not able to complete the blood meal (8 from *dsLIPS-1* + *dsLIPS-2* and 3 from *dsLIPS-2*-injected females), and therefore, the sample dimensions vary between the tests. Letters (A and B) denote groups with similar (same letter) or different means, as determined by statistical tests. Schemes were created as in Figure 1A. See also Figure S2 and Video S1..

intradermal probing after the proboscis has anchored to the skin.[40] We also observed that stimulated mosquitoes started secreting saliva—visible as discarded drop of fluid at the tip of the stylet—suggesting that either LIPS-2 directly or the probing movements stimulated by LIPS-2 cause salivation.

Notably, dsLIPS-2-injected mosquitoes probe and feed for the same amount of time on membrane-covered heparinized blood compared with control (i.e., dsGFP injected) females, similarly to what was described in salivary duct transacted females[15] (Figure S2). Taken together, these data suggest that LIPS-2 might be necessary to sustain salivation, which in turn shortens the intradermal probing.

This observation led us to hypothesize that LIPS-2 could interact with one specific mouthpart composing the stylet. We therefore generated a GFP-fused albLIPS-2 variant (Figure S3) and observed the localization of fluorescence upon stimulation of mosquitoes. By incubating the dissected stylets with the GFP-albLIPS-2, fluorescent signals localized at the very end tip of the labrum only (Figure 3B), at the opening of the food channel. Of note, live mosquitoes stimulated by the GFP-fused protein started consuming the mixture, as visible by fluorescent signals in the proboscis and in the crop located in the abdomen, whereas mosquitoes stimulated with GFP did not ingest any protein (Figure S3). These data suggest that the LIPS-2-induced stimulus also causes the consumption of the protein solution. We further demonstrated that this process is reversible and dependent on the LIPS-2 probing trigger: mosquito females exposed to albLIPS-2 and extensively washed in PBS, indeed, rapidly ceased to probe; probing quickly restarted as soon as the mosquitoes were re-exposed to albLIPS-2 (Video S3).

Notably, the mosquito labrum carries two lateral nerve canals that converge at the distal end of the organ (Figure 3C). Although only few cell nuclei are visible at the tip of the labrum, multiple dendrites have been described, forming, at the very end tip, two types of labral sense organs.[43] There are four thick-walled chemoreceptors, presenting with five dendrites and a pore on the cuticle surface, most likely used to detect blood or its components. Of these four chemoreceptors, two occur at the labral tip forming the apical sensilla and the other two are located at short distance along the lateral side of the labrum, named the subapical sensilla. In addition to this type of sense organ, there are two dendrites known as labral ridge receptors (lrr) located inside the V-shaped labral ridges; these are tactile receptors with proprioceptive function, giving information about labrum position and bending during feeding.[43] As LIPS-2 stimulates mosquito probing, we hypothesized that the signal might involve these latter tactile dendrites. We therefore investigated if LIPS-2 in the mosquito saliva might exert gross morphological

Please cite this article in press as: Arnoldi et al., A salivary factor binds a cuticular protein and modulates biting by inducing morphological changes in the mosquito labrum, Current Biology (2022), https://doi.org/10.1016/j.cub.2022.06.049

CellPress
OPEN ACCESS

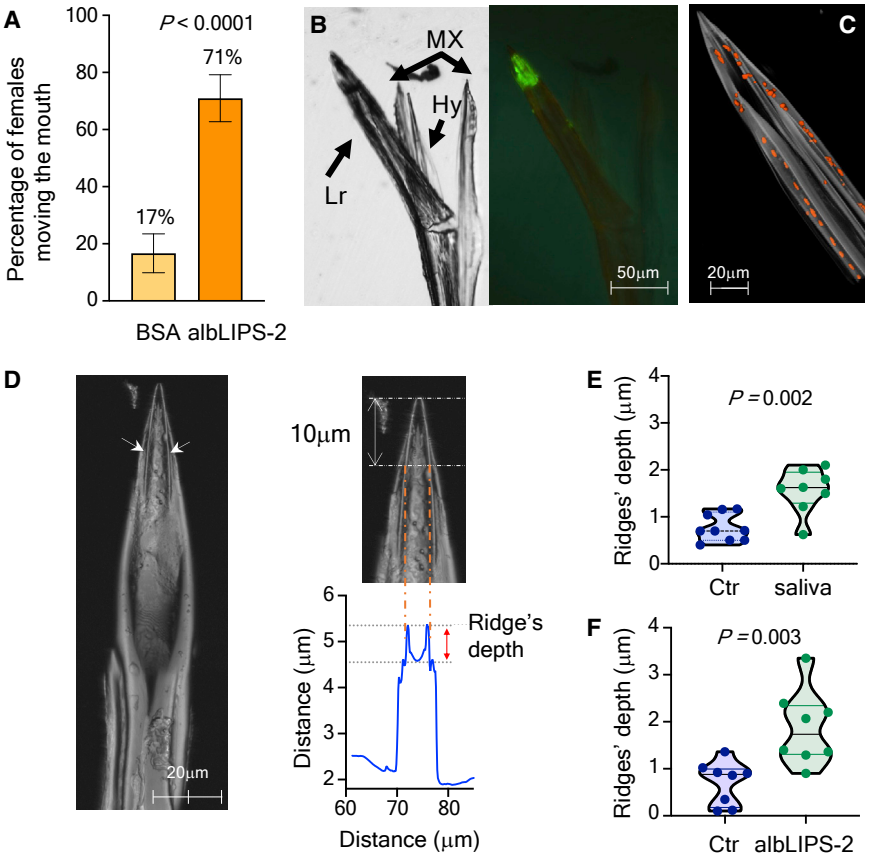

Figure 3. LIPS-2 binds the mosquito labrum and induces biting movements

(A) Recombinant albLIPS-2 (1 mg mL^{-1}) induces probing movements in mosquitoes (70.97% ± 8.2%; n = 31) whose stylet has been exposed for 30 s to the protein mixture compared with mosquitoes exposed to BSA (16.67% ± 6.8%; n = 30). Based on the amount of salivary proteins that we collected in previous experiments (Figure 1) and what has been also reported,[17,41,42] we calculated that the total protein quantity in saliva is about 30–120 mg mL^{-1} and that 1 mg mL^{-1} could be a good proxy of LIPS-2 concentration in the saliva, considering the relative amount of spots in 2D gel analysis (Figure 1). Furthermore, we chose 30 s exposure considering that mosquitoes likely salivate during the period of the intradermal probing (22 s mean; Figure 2) but that during our exposure experiments, more time is needed to make the stylet fully immersed in the protein solution to reach the tip of the labrum, which is masked by the other components of the stylet. p value is from Fisher's exact test; the percentage of the proportion is reported for each class with its associated standard deviation. The odds ratio (OR) between the albLIPS-2 and the BSA group is 12.25 ($CI_{95\%}$ = 3.57–42.09).

(B) Widefield (left) and fluorescence (right) picture of stylet exposed to recombinant GFP-albLIPS-2 protein, with the different parts of the stylet successively separated with a tweezer. Lr, labrum; Mx, maxillae; Hy, hypopharynx. LIPS-2 interacts specifically with the tip of the labrum, as visible by the intense green, fluorescent signal. See also Figure S3 and Videos S2 and S3.

(C) 3D reconstruction using 3D Slicer of the position of cell nuclei in the mosquito labrum, after fluorescence confocal analysis. Nuclei have been stained with DAPI and pseudo-colored in red, whereas the strong autofluorescence of chitin has been acquired in the green channel and pseudo-colored in gray.

(D) Laser scanning confocal microscopy of the *Ae. albopictus* labrum. The depth of the V-shaped ridges (white arrows in the figure) was calculated as the difference between the tip of the ridge and the bottom of the concavity between the two ridges at 10 μm from the tip of the labrum. The figure shows a labrum from the treated group. The graph shows the distance of the labrum from the bottom of the slide (y axes) at 10 μm from the tip. The x axis reports the distance (μm) of the object from the left edge of the field analyzed.

(E) Mosquitoes salivating in a "bite-blot" experiment showed taller V-shaped ridges than labra from not-salivating mosquitoes (median salivating = 1.62 μm; median controls = 0.70 μm; Mann-Whitney U = 6; p = 0.002). See also Figure S3.

(F) albLIPS-2 treated labra showed taller ridges than control labra (median albLIPS-2 treated = 1.74 μm; median controls = 0.88 μm; Mann-Whitney U = 5; p = 0.003).

changes at the tip of the labrum, possibly stimulating the proprioceptive neurons.

LIPS-2 binding induces a change in the labrum tip morphology

We analyzed the morphology of the labrum using a confocal laser scanning microscope (CLSM) (Figure 3D), focusing our attention at the labrum ventral side, which is the first component contacting the host skin. We noticed that mosquitoes naturally salivating in a bite-blot experiment[32] showed a change in the depth of the labrum's V-shaped ridges, characteristic of the tip of the labrum containing the lrr, compared with non-salivating mosquitoes (Figure 3E); this change is not visible in LIPS-2 knockdown mosquitoes (Figure S3). In particular, labra treated with recombinant albLIPS-2 showed a mean increase of 0.8 μM in the depth of the V-shaped ridges compared with controls (Figure 3F). These results further highlight the role of LIPS-2 as a major factor responsible for the morphological change in the labrum that might be sensed by tactile dendrites.

LIPS-2 interacts with the cuticular protein Cp19

To identify the possible molecular interactor of LIPS-2 on the mosquito labrum, we wondered whether this protein could interact with specific receptors located on the cuticle of the V-shaped ridges or with non-protein components. Pre-treatment of mosquito proboscis with trypsin strongly affected the fluorescence localization of GFP-albLIPS-2 at the proboscis' tip (Figure 4A), suggesting that LIPS-2 interacts with a proteinaceous receptor. We then dared to probe the identity of this protein interactor, making few considerations: (1) the region is small and highly rich in cuticle, whose components are usually highly cross-linked by laccases,[44] limiting the effectiveness of classical proteomic studies, and (2) most of the labrum cells are neurons with only few dendrites innervating the region. We therefore hypothesized that the LIPS-2 interactor might be a surface protein

Please cite this article in press as: Arnoldi et al., A salivary factor binds a cuticular protein and modulates biting by inducing morphological changes in the mosquito labrum, Current Biology (2022), https://doi.org/10.1016/j.cub.2022.06.049

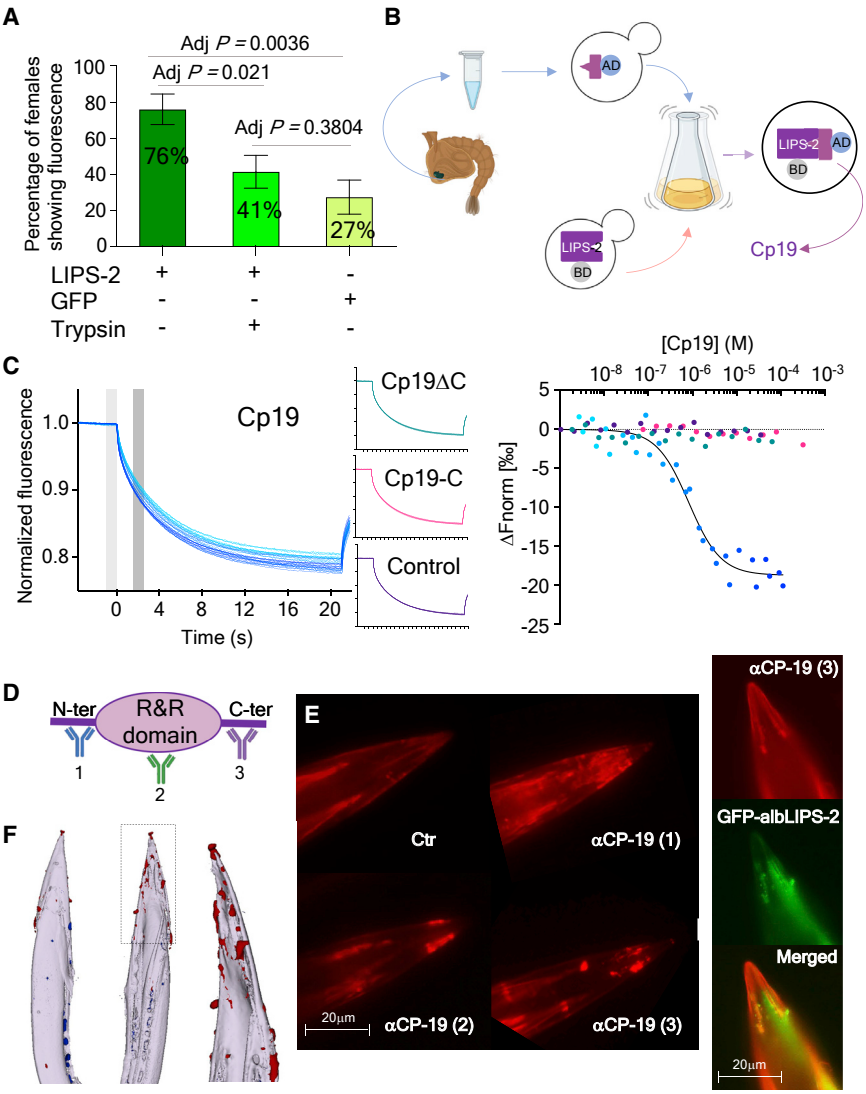

Figure 4. LIPS-2 interacts with Cp19 at the tip of the mosquito labrum

(A) The interaction with the mosquito labrum is protein mediated, as pre-treatment of stylets with trypsin (1 mg mL^{-1} h^{-1}) causes a reduction of the proportion of stylets with green signal after exposure with albLIPS-2 (GFP-albLIPS-2, 76.00% ± 8.5%, n = 25; trypsin treatment and GFP-albLIPS-2, 41.38% ± 9.1%, n = 29; GFP, 27.27% ± 9.5%, n = 22). p values are from Fisher's exact test corrected with false discovery rate to correct for multiple testing (adj p); the percentage of the proportion is reported for each of the three groups with its associated standard deviation.

(B) Schematic representation of the yeast two-hybrid screening procedure. Labra from 100 pupae, the majority of which within 24 h from pupation, were dissected and the extracted RNA was used to build a prey cDNA library cloned in pGADT7-Rec plasmid and transformed into the Y187 *Saccharomyces cerevisiae* strain, generating 2 × 10^5 independent clones. *LIPS-2* was used as bait and cloned in the pGBKT7 plasmid in the Y2HGold *S. cerevisiae* strain. Mating between the strains has been induced and the diploid cells selected using proper culturing plates. We reached 14.5% of mating efficiency, testing 3.5 × 10^6 possible interactions, and obtaining about 10^3 positive clones. Of the 150 screened, some carried a portion of the Cp19 gene. Schemes created as in Figure 1A. See also Figure S4 and Data S1.

(C) MST analysis of the interaction between Cp19 and GFP-albLIPS-2. The difference in fluorescence was calculated using the T-jump interval (1.5–2.5 s, dark gray). The MST traces are shown for the experiment using 20 nM GFP-albLIPS-2 and a serial dilution of the Cp19 protein, indicated with the blue scale (from blue to light blue). Control, GFP-labeled control protein; Cp19Δ, Cp19 deprived of the C-terminal sequence (aa 86–104); Cp19-C, *in vitro* synthetized Cp19 C-terminal peptide. See also Figure S4.

(D) Schematic representation of the domain organization of the Cp19 protein. The position of the epitopes against which the antibodies have been raised is also shown.

(D) Immunofluorescence (left) staining and co-immunolocalization (right) using anti-Cp19 antibodies. The three antibodies show similar patterns on the tip of the mosquito labrum and the signal using the antibody #3 co-localizes with the GFP-albLIPS-2. See also Figure S4.

(E) Confocal microscopy and 3D reconstruction of labrum showing Cp19 localization (red). The signal is on the ventral surface (central and right panel), and it is not present on the dorsal surface.

constituting the cuticle possibly produced during formation of the mosquito labrum at the pupal stage. We extracted RNA from pupal female labra and built a library of labrum prey proteins for yeast two-hybrid screening (Y2H; Figures 4B and S4). Using LIPS-2 as bait protein, we found a clone expressing the C-terminal portion (aa 75–104) of one bona fide interactor, which is a cuticular protein (Cp19; Data S1). Cp19 is a cuticular protein predicted to belong to the RR (Rebers and Riddiford Consensus)-2 family that are often found in the hard cuticle or in the insect exocuticle.[45] Computational protein modeling[46] suggests that RR-2 proteins likely have a central core composed of antiparallel β sheets, which interacts with the chitin, and N- and C-terminal disordered regions protruding outside the cuticle's surface. Suggestively, the Y2H clones carried the Cp19 C-terminal region.

The LIPS-2/Cp19 interaction could be confirmed in yeast using a clone containing the full-length coding sequence of the *Cp19* gene without the putative signal peptide (aa 1–17) and swapping prey and bait genes. The co-expression of the fusion proteins in yeasts was also confirmed by western blot analysis (Figure S4). The interaction was further validated using a microscale thermophoresis (MST) approach using GFP-albLIPS2 (Figure 4C). The dissociation constant for the full-length, recombinant Cp19 was 800 nM; no interaction could be detected between Cp19 and a control GFP-labeled protein, indicating that the interaction does not involve contacts with the GFP tag and that it is Cp19-specific. Notably, Cp19ΔC fragments deprived of the C-terminal sequence originally present in the Y2H clone (aa 86–104) do not interact with

GFP-albLIPS-2, confirming that the C-terminal region is essential to establish the interaction. Surprisingly, no interaction could be detected with a synthetic Cp19 C-terminal peptide (Cp19-C), suggesting that more extended contacts with the Cp19 core are required for LIPS-2 binding. This is supported by the reconstituted LIPS-2 binding obtained by mixing Cp19ΔC and Cp19-C (Figure S4).

To further confirm that the LIPS-2:Cp19 interaction occurs at the tip of the mosquito labrum, we probed the location of Cp19. We generated three distinct Cp19-specific antibodies recognizing different protein epitopes (Figure 4D). Immunofluorescence analysis confirmed that Cp19 co-localizes on the ventral side of the labrum, in the same region where we detected the LIPS-2 binding (Figure 4E) and that Cp19 is exposed to the ventral surface of the tip of the labrum (Figure 4F)

As hypothesized when searching for a possible LIPS-2 interactor, qPCR analysis revealed that the Cp19 gene is expressed at high levels in the labra during pupal development, with a peak around 24 h after pupation (Figure S4). Western blot analysis on adult labra further suggests that the Cp19 is heavily cross-linked to other cuticle components (Figure S4). Interestingly, no expression of the orthologous gene and no Cp19 protein was detected in the labra of anophelines (*Anopheles stephensi*), suggesting that the LIPS-2:Cp19 interaction likely evolved after the splitting of Culicinae from Anophelinae and opening the question whether an analogous system has evolved in *Anopheles* mosquitoes.

Considering the uniqueness of LIPS-2 protein, with a key role in regulating *Aedes* feeding processes, we then investigated the molecular and structural features of this protein in relation to its biological role.

Structural characterization of LIPS reveals a possible binding site for Cp19

Purified albLIPS-2 is monomeric *in solution*, as determined using size-exclusion chromatography directly coupled with small-angle X-ray scattering (SEC-SAXS) (Figure S5A; Table S2), with an all-alpha helical secondary structure organization as suggested by circular dichroism (Figure S5B). The protein could be crystallized (Figure S5C), and its 2.2-Å resolution molecular structure was determined using single-wavelength anomalous dispersion (SAD) using selenomethionine derivatization (Table S3). The structure revealed a new folding topology, characterized by two consecutive domains entirely composed of α helices (Figure 5A). The N-terminal domain features a compact helical bundle (CHB), connected to a C-terminal domain with α helices arranged in short helix-turn-helix motifs (HTH) (Figures 5A and 5B). Average B-factors for the two domains were 74.89 and 49.66 $Å^2$, respectively. The increased flexibility observed in the CBH domain was mostly due to two-solvent-exposed loops, connecting residues 46–54 and residues 82–95 (Figure S6A). Two disulphide bonds, whose presence was expected by comparative SDS-PAGE performed in reducing and non-reducing conditions (Figure S6B), stabilize the protein structure. Treatment of the salivary glands extracts with PNGase suggested that native LIPS-2 is glycosylated, possible with paucimannose glycans, typical of insect cells (Figure S6C). The two asparagine residues predicted to be glycosylated (Asn168 and Asn175, respectively) are proximate to the convex interface between the two domains (Figure S6), suggesting a possible non-essential role in further stabilizing the protein structure. Notably, Asn168 is one of the few surface residues displaying high conservation in LIPS sequences from different species (Figures S5D and S5E). Comparison between the crystal structure and SEC-SAXS solution data yielded remarkably consistent results (Figure S6D), suggesting absence of crystallization-induced artifacts affecting the albLIPS-2 molecular architecture.

The analysis of the protein structure ruled out any potential enzymatic functions and probing of the albLIPS-2 surface did not suggest clear presence of cavities suitable for binding of small molecule ligands. However, the peculiar 3D architecture, particularly that of the N-terminal CHB domain, is reminiscent of hormone-like polypeptides, further suggesting that it might work as docking module for macromolecular interactions.

Considering the relatively limited degree of amino acid sequence conservation (<60% identity; Figure S5D and S5E) in LIPS gene products among multiple mosquito species, we wondered whether this could have an impact on their tertiary structure. Computational modeling of homologous LIPS from *Ae. aegypti* (aeLIPS-2) and *Ochlerotatus* (*Aedes*) *triseriatus* (trisLIPS-2) consistently suggested very similar three-dimensional organizations for these proteins, supporting the idea that despite sequence divergence, the LIPS fold could constitute a functional hallmark of this protein class (Figure S5F).

To map the interaction site between LIPS-2 and Cp19, we performed a test based on the "absence of interference" using yeasts.[47] We generated a library of mutant LIPS-2 proteins using error-prone PCR, and we screened the clones that retained their ability to interact with Cp19 (Data S2). This approach indicated that the LIPS-2 N-terminal CHB domain is responsible for the interaction with Cp19, which was further validated *in vitro* using MST (Figure 5D). The dissociation constant for the isolated N-terminal CBH domain was 14 nM; this value is, however, not directly comparable with what assessed for full-length LIPS-2, as binding of Cp19 to full-length LIPS-2 causes a variation in the T-jump region of the MST traces (1.5–2.5 s), whereas binding of Cp19 to LIPS-2 CHB domain causes a variation more clearly detectable in the thermophoresis region (14.5–15 s). Such observations support the possibility that the presence of the C-terminal HTH domain affects either the overall folding of the mature LIPS-2 protein or its overall affinity Cp19, possibly by shielding a non-specific contact surface exposed in the recombinantly produced isolated CHB domain.

By analyzing the mutations obtained through the "absence of interference" approach and the LIPS- amino acid conservation among *Aedes* and *Culex* mosquitoes (Figure S5), we identified a conserved surface patch formed by residues V29, S30, E32, L34, I37, R38, K108, and F113, which might be putatively involved in this interaction (Figure 5C). We therefore generated a LIPS-2 mutant (GFP-albLIPS-2(R38S)) that heavily alters the electrostatic environment of this region; MST experiments using GFP-albLIPS-2(R38S) showed that this amino acid change dramatically reduces the interaction between LIPS-2 and Cp19, although a control mutant (GFP-albLIPS-2(S151A; R152S)) showed a dissociation constant compatible with that of the wild-type protein, when the MST traces are evaluated in the T-jump region (770 nM) (Figure 5D).

Please cite this article in press as: Arnoldi et al., A salivary factor binds a cuticular protein and modulates biting by inducing morphological changes in the mosquito labrum, Current Biology (2022), https://doi.org/10.1016/j.cub.2022.06.049

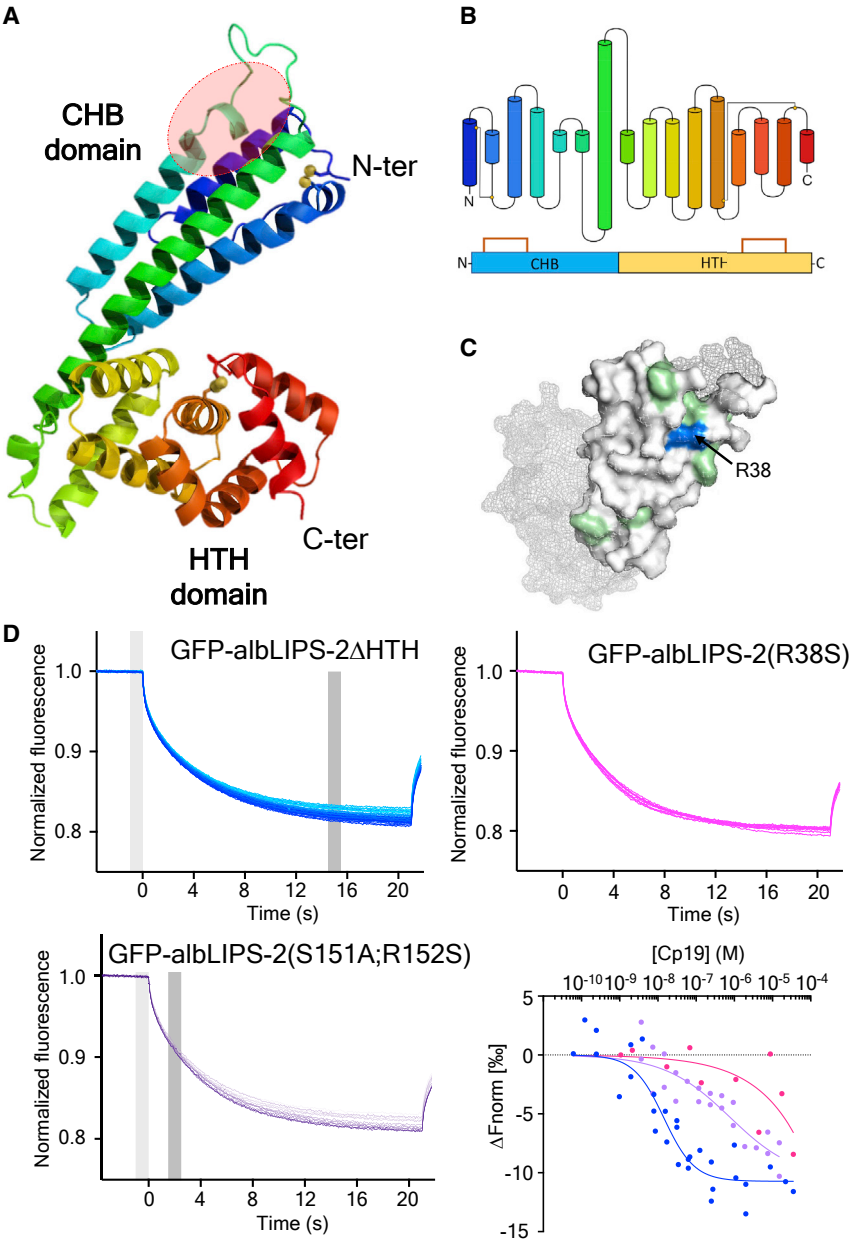

Figure 5. Structural characterization of albLIPS-2

(A) Cartoon representation of albLIPS-2 molecular structure, rainbow colored from the N terminus (blue) to the C terminus (red). The two disulfide bridges interlocking the N-terminal compact helical bundle (CHB) domain and the C-terminal helix-turn-helix (HTH) domain are highlighted with yellow spheres. The red circle indicates the putative Cp19 interacting region. See also Tables S2 and S3 and Figures S5 and S6.

(B) Schematic representation of the secondary structure (top) and domain organization (bottom) of the albLIPS-2 protein, with the α helices represented as pipes and disulphide bridges shown as connecting lines between the helices. See also Figures S5 and S6.

(C) Identification of the putative Cp19 binding surface of the albLIPS-2 protein at the top of the CHB domain (shown as surface); the C-terminal HTH domain is indicated with a transparent mesh. Conserved CHB residues are shown in green. Residue Arg38 is shown in blue, and it has been selected for mutagenesis. See also Data S2.

(D) MST analysis of GFP-albLIPS-2ΔHTH, GFP-albLIPS-2(R38S), and GFP-albLIPS-2(S151A; R152S) binding to Cp19. Changes in fluorescence were analyzed either in the T-jump (1.5–2.5 s) or in the thermophoresis region (14.5–15.5 s, dark gray).

DISCUSSION

Engorging the blood of a vertebrate host is a key step during the mosquito life cycle and for the transmission of multiple mosquito-borne pathogens. What occurs during this short timeframe in a very narrow space shapes the life of billions of people every day.[2] Mosquito saliva has a key role in regulating the interaction between the mosquito vectors, the vertebrate hosts, and the pathogens.[5,6,8–15,22,23,33,48,49] Using an integrative approach combining *in vitro* molecular and structural biology with *in vivo* and *ex vivo* studies, we have identified a novel role for mosquito saliva, serving as a vector-to-vector signal regulating the initial phases of the biting process. We have found the LIPS-Cp19 axis as the initial trigger of this unprecedented signaling pathway in *Aedes* mosquitoes.

LIPS-2 are female-specific salivary factors that can bind the tip of the mosquito labrum by interacting with the cuticular protein Cp19. Particularly, this interaction occurs on and proximate to a labral cuticular structure known as V-shaped ridges, causing a morphological change in the depth of these ridges. Of note, these cuticular architectures accommodate the dendrites of tactile neurons involved in proprioception,[43] which might feel these changes, promoting in turn probing and salivation.

In our model (Figure 6), mosquitoes salivate soon after landing to the skin, when they push their proboscis on the skin surface before penetrating it. Salivation, in turn, induces changes at the V-shaped ridges of the labrum, inducing further salivation and enhancing the speed of intradermal probing. These changes are fully reversible, as intense backwashes of LIPS-2-stimulated mosquitoes stop probing and salivating (Video S3): in this context, we speculate that the flow of the host blood might scrape the LIPS-2 from the stylet, thereby switching from intradermal probing to the subsequent blood feeding phase.

Interestingly, cuticular proteins are also key constituents of the tip of the mouth apparatus of other piercing-sucking insects, the aphids, which feed on plants and can transmit plant viruses.[50–55] In these insects, the tip of the maxillary stylet hosts a structure known as acrostyle with high concentration of cuticular proteins. Some viruses can interact with these proteins to ensure

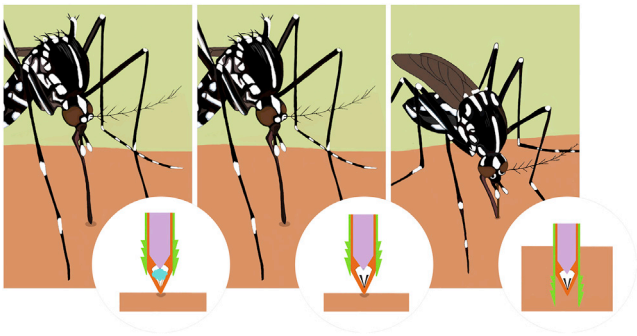

Figure 6. Model of the role of LIPS-2 during blood feeding

Mosquitoes start salivating when they press the proboscis on the skin surface (left panel), since the saliva is deposited on the surface of the membrane during bite-blot experiments.[32] The LIPS-2 in the saliva binds the Cp19 at the tip of the labrum and this causes a change in the morphology of the V-shaped ridges, enhancing their depth (central panel). Finally, this change is sensed by mosquitoes, and it causes further salivation and the beginning of the intradermal probing (right panel), facilitating blood vessel location. The labrum is shown in orange, the hypopharynx carrying the salivary duct and its opening at the tip in violet, and maxillae in green. The V-shaped ridges are shown as black line after stimulation.

plant-to-plant mechanical transmission. Suggestively, previous studies demonstrated that *Aedes* mosquitoes can mechanically or passively transmit not only lumpy skin disease virus,[56] but also arboviruses with a predominant biological transmission, such as the chikungunya, West Nile, and Zika.[57–59] This type of transmission seems to be short lasting, i.e., it occurs mostly within 1 h from an infectious blood meal. This transmission mode acquires significance by considering the feeding behavior of *Aedes* females: to reach satiety in natural contexts, they usually bite different people in a short period of time.[2] Notably, one of the Cp19 orthologs in *Aedes aegypti* has been demonstrated to bind the envelope proteins of West Nile and Dengue viruses,[60] opening the possibility that this interaction might occur at the tip of the labrum favoring the passive transmission of the virus. This phenomenon has important implications for vectorial capacity, particularly in non-endemic areas and during local outbreaks.

Generally, these data point out to a possible, unexplored role of cuticular proteins in insect mouth, acting as hotspots for molecular interaction with insect's and pathogen's factors affecting both biting behavior and vector competence.

Noteworthy, LIPS proteins constitute a novel protein folding family with two distinct domains, both entirely constituted by α helices. The Cp19 interaction occurs exclusively at the N-terminal CHB domain, leaving additional possible functional roles to the C-terminal domain, also considering its higher degree of amino acid sequence conservation. Indeed, mosquito salivary proteins have shown pleiotropic functions.[49]

The absence of *LIPS* orthologous genes in anopheline species opens the possibility that homologous functions as probing stimulators might be exerted by different and completely unrelated factor(s). Likewise, considering that Cp19-like proteins have not been detected in the labrum of *Anopheles* mosquitoes, the whole LIPS-Cp19 axis may be replaced by different actors. Indeed, several yet uncharacterized factors present in anophelines are absent in aedines and vice versa, suggesting that similar functions might be exerted by completely unrelated proteins through functional convergent evolution. The fine details underlying this feedback mechanism in these and possibly also in other insect vectors (e.g., aphids) demand further investigation as well as the possible additional modulators involved in this process.

A better characterization of the interactions occurring at the mosquito bite microenvironment will not only widen our understanding of this unique biological process, but it might provide unprecedented insights about vector competence and for the design of future strategies to reduce the burden associated to mosquito-borne diseases.

STAR★METHODS

Detailed methods are provided in the online version of this paper and include the following:

- KEY RESOURCES TABLE
- RESOURCE AVAILABILITY
  - Lead contact
  - Materials availability
  - Data and code availability
- EXPERIMENTAL MODEL AND SUBJECT DETAILS
- METHOD DETAILS
  - Insect rearing
  - Sample preparation for proteomics analysis
  - LC-MS/MS Analysis
  - Deglycosylation assay
  - *In vivo* RNA-interference (RNAi)
  - Gene expression analysis by RT-qPCR
  - Behavioral assay
  - Yeast two-hybrid screening
  - Co-transformation and autoactivation assays
- RANDOM MUTAGENESIS OF LIPS-2 COUPLED TO Y2H
  - Western blot analysis
  - Immunofluorescence assays
  - Protein expression and purification
  - Laser scanning confocal microscopy
  - Generation of LIPS-2 mutants
  - Protein unfolding resistance measurements
  - Circular Dichroism (CD)
  - SEC-SAXS
  - X-ray data collection and processing
  - Structure determination and refinement
  - Evaluation of LIPS-mosquito interactions
  - MST analysis of protein-protein interaction
- QUANTIFICATION AND STATISTICAL ANALYSIS

SUPPLEMENTAL INFORMATION

Supplemental information can be found online at https://doi.org/10.1016/j.cub.2022.06.049.

ACKNOWLEDGMENTS

We thank Prof. A.R. Malacrida and Prof. G. Gasperi for inspiring discussions and support throughout project development, Prof. Pasquale Vena for its support during laser confocal microscopy studies, Dr. G. Barbieri for her support

during LIPS-2 mutagenesis, and Dr. V. Rao for his help in the collection of mosquito saliva. We thank the European Synchrotron Radiation Facility (ESRF) and the Swiss Light Source (SLS) for the provision of synchrotron radiation and infrastructure support. We also thank the PASS-BioMed Facility (Centro Grandi Strumenti) at the University of Pavia and the Unitech NoLIMITS Facility at the University of Milan for the provision of microscope infrastructure and the associated technical support. This project has received funding from Fondazione Cariplo (2017-0798 to P.G.), the NATO Science for Peace and Security Program (no. SPS.MYP G5071 to F.F.), the Giovanni Armenise-Harvard Foundation (CDA2013 to F.F.), the Italian Ministry of Education, University and Research (MIUR) through a "PRIN" grant (n. 2017RPHBCW to F.F.), and the Dipartimenti di Eccellenza Program (2018–2022, to the Department of Biology and Biotechnology "L. Spallanzani," University of Pavia). None of the funding sources had roles in study design, collection, analysis, and interpretation of data, in the writing of the report, and in the decision to submit this article for publication.

AUTHOR CONTRIBUTIONS

I.A. performed Y2H screenings, cloning, and microscopy studies. G.M. purified proteins and used MST to study protein-protein interactions. D.G. and L.D. helped in acquiring laser confocal microscopy data and their analysis. C.B. helped in designing and performing epPCR. P.G., M.F., M.D.V., and P.I. carried out 2D-gel experiments and associated analyses. P.G. and M.F. performed mass spectrometry experiments, with support from P.I. P.G. performed collection of the mosquito saliva and salivary glands dissections; he performed the knockdown experiments and their associated analysis. P.G., with the support of F.F., purified LIPS-2 and the GFP-fused variant, crystallized albLIPS-2, and performed the behavioral experiments with the purified proteins. P.G. and F.F. determined LIPS-2 molecular structure and carried out refinement and crystallography analyses. P.G. and F.F. designed the study, analyzed results, and wrote the paper, with substantial contributions from all the authors.

DECLARATION OF INTERESTS

The authors declare no competing interests.

Received: January 19, 2022
Revised: May 23, 2022
Accepted: June 15, 2022
Published: July 13, 2022

REFERENCES

1. Castro, M.C., Wilson, M.E., and Bloom, D.E. (2017). Disease and economic burdens of dengue. Lancet Infect. Dis. *17*, e70–e78.
2. WHO (2020). Vector-borne diseases. https://www.who.int/news-room/fact-sheets/detail/vector-borne-diseases.
3. Kramer, L.D., and Ciota, A.T. (2015). Dissecting vectorial capacity for mosquito-borne viruses. Curr. Opin. Virol. *15*, 112–118.
4. Cantillo, J.F., Fernández-Caldas, E., and Puerta, L. (2014). Immunological aspects of the immune response induced by mosquito allergens. Int. Arch. Allergy Immunol. *165*, 271–282.
5. Hudson, A., Bowman, L., and Orr, C.W. (1960). Effects of absence of saliva on blood feeding by mosquitoes. Science *131*, 1730–1731.
6. Schneider, C.A., Calvo, E., and Peterson, K.E. (2021). Arboviruses: how saliva impacts the journey from vector to host. Int. J. Mol. Sci. *22*, 9173.
7. Ribeiro, J.M., Mans, B.J., and Arcà, B. (2010). An insight into the sialome of blood-feeding Nematocera. Insect Biochem. Mol. Biol. *40*, 767–784.
8. Guerrero, D., Cantaert, T., and Missé, D. (2020). *Aedes* mosquito salivary components and their effect on the immune response to arboviruses. Front. Cell. Infect. Microbiol. *10*, 407.
9. Hastings, A.K., Uraki, R., Gaitsch, H., Dhaliwal, K., Stanley, S., Sproch, H., Williamson, E., MacNeil, T., Marin-Lopez, A., Hwang, J., et al. (2019). *Aedes aegypti* NeSt1 protein enhances Zika virus pathogenesis by activating neutrophils. J. Virol. *93*. e00395–19.
10. Sri-In, C., Weng, S.C., Chen, W.Y., Wu-Hsieh, B.A., Tu, W.C., and Shiao, S.H. (2019). A salivary protein of *Aedes aegypti* promotes dengue-2 virus replication and transmission. Insect Biochem. Mol. Biol. *111*, 103181.
11. Surasombatpattana, P., Ekchariyawat, P., Hamel, R., Patramool, S., Thongrungkiat, S., Denizot, M., Delaunay, P., Thomas, F., Luplertlop, N., Yssel, H., and Misse, D. (2014). *Aedes aegypti* saliva contains a prominent 34-kDa protein that strongly enhances dengue virus replication in human keratinocytes. J. Invest. Dermatol. *134*, 281–284.
12. Chuang, Y.M., Agunbiade, T.A., Tang, X.D., Freudzon, M., Almeras, L., and Fikrig, E. (2021). The effects of a mosquito salivary protein on sporozoite traversal of host cells. J. Infect. Dis. *224*, 544–553.
13. Schleicher, T.R., Yang, J., Freudzon, M., Rembisz, A., Craft, S., Hamilton, M., et al. (2018). A mosquito salivary gland protein partially inhibits *Plasmodium* sporozoite cell traversal and transmission. Nat. Commun. *9*, 2908.
14. Schneider, B.S., Mathieu, C., Peronet, R., and Mécheri, S. (2011). *Anopheles stephensi* saliva enhances progression of cerebral malaria in a murine model. Vector Borne Zoonotic Dis. *11*, 423–432.
15. Ribeiro, J.M., Rossignol, P.A., and Spielman, A. (1984). Role of mosquito saliva in blood vessel location. J. Exp. Biol. *108*, 1–7.
16. Yamamoto, D.S., Sumitani, M., Kasashima, K., Sezutsu, H., and Matsuoka, H. (2016). Inhibition of malaria infection in transgenic anopheline mosquitoes lacking salivary gland cells. PLoS Pathog. *12*, e1005872.
17. Li, Z., Soohoo-Hui, A., O'Hara, F.M., and Swale, D.R. (2022). ATP-sensitive inward rectifier potassium channels reveal functional linkage between salivary gland function and blood feeding in the mosquito. *Aedes aegypti*. Commun. Biol. *5*, 278.
18. Labuda, M., and Kozuch, O. (1989). Amplification of arbovirus transmission by mosquito intradermal probing and interrupted feeding. Acta Virol. *33*, 63–67.
19. Rossignol, P.A., Ribeiro, J.M., and Spielman, A. (1984). Increased intradermal probing time in sporozoite-infected mosquitoes. Am. J. Trop. Med. Hyg. *33*, 17–20.
20. Ribeiro, J.M. (2000). Blood-feeding in mosquitoes: probing time and salivary gland anti-haemostatic activities in representatives of three genera (*Aedes, Anopheles, Culex*). Med. Vet. Entomol. *14*, 142–148.
21. Law, J.H., Ribeiro, J.M., and Wells, M.A. (1992). Biochemical insights derived from insect diversity. Annu. Rev. Biochem. *61*, 87–111.
22. Islam, A., Emran, T.B., Yamamoto, D.S., Iyori, M., Amelia, F., Yusuf, Y., Yamaguchi, R., Alam, M.S., Silveira, H., and Yoshida, S. (2019). Anopheline antiplatelet protein from mosquito saliva regulates blood feeding behavior. Sci. Rep. *9*, 3129.
23. Conway, M.J. (2021). Type I hypersensitivity promotes *Aedes aegypti* blood feeding. Sci. Rep. *11*, 14891.
24. Battaglia, V., Gabrieli, P., Brandini, S., Capodiferro, M.R., Javier, P.A., Chen, X.G., Achilli, A., Semino, O., Gomulski, L.M., Malacrida, A.R., et al. (2016). The worldwide spread of the tiger mosquito as revealed by mitogenome haplogroup diversity. Front. Genet. *7*, 208.
25. Jourdain, F., Roiz, D., de Valk, H., Noël, H., L'Ambert, G., Franke, F., Paty, M.C., Guinard, A., Desenclos, J.C., and Roche, B. (2020). From importation to autochthonous transmission: drivers of chikungunya and dengue emergence in a temperate area. PLOS Negl. Trop. Dis. *14*, e0008320.
26. Arcà, B., Lombardo, F., Francischetti, I.M., Pham, V.M., Mestres-Simon, M., Andersen, J.F., and Ribeiro, J.M. (2007). An insight into the sialome of the adult female mosquito *Aedes albopictus*. Insect Biochem. Mol. Biol. *37*, 107–127.
27. Boorman, J. (1987). Induction of salivation in biting midges and mosquitoes, and demonstration of virus in the saliva of infected insects. Med. Vet. Entomol. *1*, 211–214.
28. Barredo, E., and DeGennaro, M. (2020). Not just from blood: mosquito nutrient acquisition from nectar sources. Trends Parasitol. *36*, 473–484.

29. Marinotti, O., James, A.A., and Ribeiro, J.C. (1990). Diet and salivation in female *Aedes aegypti* mosquitoes. J. Insect Physiol. *36*, 545–548.

30. Peng, Z., Caihe, L., Beckett, A.N., Guan, Q., James, A.A., and Simons, F.E. (2016). rAed a 4: a new 67-kDa *Aedes aegypti* mosquito salivary allergen for the diagnosis of mosquito allergy. Int. Arch. Allergy Immunol. *170*, 206–210.

31. Jones, J.C., and Pilitt, D.R. (1973). Blood-feeding behavior of adult *Aedes aegypti* mosquitoes. Biol. Bull. *145*, 127–139.

32. King, J.G., Vernick, K.D., and Hillyer, J.F. (2011). Members of the salivary gland surface protein (SGS) family are major immunogenic components of mosquito saliva. J. Biol. Chem. *286*, 40824–40834.

33. Sun, P., Nie, K., Zhu, Y., Liu, Y., Wu, P., Liu, Z., Du, S., Fan, H., Chen, C.H., Zhang, R., et al. (2020). A mosquito salivary protein promotes Flavivirus transmission by activation of autophagy. Nat. Commun. *11*, 260.

34. Conway, M.J., Londono-Renteria, B., Troupin, A., Watson, A.M., Klimstra, W.B., Fikrig, E., and Colpitts, T.M. (2016). *Aedes aegypti* D7 saliva protein inhibits dengue virus infection. PLoS Negl. Trop. Dis. *10*, e0004941.

35. Doucoure, S., Cornelie, S., Patramool, S., Mouchet, F., Demettre, E., Seveno, M., Dehecq, J.S., Rutee, H., Herve, J.P., Favier, F., et al. (2013). First screening of *Aedes albopictus* immunogenic salivary proteins. Insect Mol. Biol. *22*, 411–423.

36. Buezo Montero, S., Gabrieli, P., Severini, F., Picci, L., Di Luca, M., Forneris, F., Facchinelli, L., Ponzi, M., Lombardo, F., and Arcà, B. (2019). Analysis in a murine model points to IgG responses against the 34k2 salivary proteins from *Aedes albopictus* and *Aedes aegypti* as novel promising candidate markers of host exposure to *Aedes* mosquitoes. PLoS Negl. Trop. Dis. *13*, e0007806.

37. Buezo Montero, S., Gabrieli, P., Montarsi, F., Borean, A., Capelli, S., De Silvestro, G., Forneris, F., Pombi, M., Breda, A., Capelli, G., and Arcà, B. (2020). IgG antibody responses to the *Aedes albopictus* 34k2 salivary protein as novel candidate marker of human exposure to the tiger mosquito. Front. Cell. Infect. Microbiol. *10*, 377.

38. Zhang, M., Zheng, X., Wu, Y., Gan, M., He, A., Li, Z., Zhang, D., Wu, X., and Zhan, X. (2013). Differential proteomics of *Aedes albopictus* salivary gland, midgut and C6/36 cell induced by dengue virus infection. Virology *444*, 109–118.

39. Wayadande, A.C., Backus, E.A., Noden, B.H., and Ebert, T. (2020). Waveforms from stylet probing of the mosquito *Aedes aegypti* (Diptera: Culicidae) measured by AC-DC electropenetrography. J. Med. Entomol. *57*, 353–368.

40. Kong, X.Q., and Wu, C.W. (2010). Mosquito proboscis: an elegant bio-microelectromechanical system. Phys. Rev. E Stat. Nonlin. Soft Matter Phys. *82*, 011910.

41. Sri-In, C., Weng, S.C., Shiao, S.H., and Tu, W.C. (2020). A simplified method for blood feeding, oral infection, and saliva collection of the dengue vector mosquitoes. PLoS One *15*, e0233618.

42. Sanchez-Vargas, I., Harrington, L.C., Black, W.C., and Olson, K.E. (2019). Analysis of salivary glands and saliva from *Aedes albopictus* and *Aedes aegypti* infected with chikungunya viruses. Insects *10*, 39.

43. Lee, R. (1974). Structure and function of the fascicular stylets and the labral and cibarial sense organs of male and female *Aedes aegypti* (L.) (Diptera, Culicidae). Quaest. Entomol. *10*, 187–215.

44. Suderman, R.J., Dittmer, N.T., Kanost, M.R., and Kramer, K.J. (2006). Model reactions for insect cuticle sclerotization: cross-linking of recombinant cuticular proteins upon their laccase-catalyzed oxidative conjugation with catechols. Insect Biochem. Mol. Biol. *36*, 353–365.

45. Vannini, L., and Willis, J.H. (2017). Localization of RR-1 and RR-2 cuticular proteins within the cuticle of *Anopheles gambiae*. Arthropod Struct. Dev. *46*, 13–29.

46. Willis, J.H., Papandreou, N.C., Iconomidou, V.A., and Hamodrakas, S.J. (2012). Cuticular proteins. In Insect Molecular Biology and Biochemistry, L.I. Gilbert, ed. (Elsevier), pp. 134–166.

47. Dhayalan, A., Jurkowski, T.P., Laser, H., Reinhardt, R., Jia, D., Cheng, X., and Jeltsch, A. (2008). Mapping of protein-protein interaction sites by the 'absence of interference' approach. J. Mol. Biol. *376*, 1091–1099.

48. Martin-Martin, I., Paige, A., Valenzuela Leon, P.C., Gittis, A.G., Kern, O., Bonilla, B., Chagas, A.C., Ganesan, S., Smith, L.B., Garboczi, D.N., and Calvo, E. (2020). ADP binding by the *Culex quinquefasciatus* mosquito D7 salivary protein enhances blood feeding on mammals. Nat. Commun. *11*, 2911.

49. Martin-Martin, I., Smith, L.B., Chagas, A.C., Sá-Nunes, A., Shrivastava, G., Valenzuela-Leon, P.C., and Calvo, E. (2020). *Aedes albopictus* D7 salivary protein prevents host hemostasis and inflammation. Biomolecules *10*, 1372.

50. Deshoux, M., Masson, V., Arafah, K., Voisin, S., Guschinskaya, N., van Munster, M., Cayrol, B., Webster, C.G., Rahbé, Y., Blanc, S., et al. (2020). Cuticular structure proteomics in the pea aphid *Acyrthosiphon pisum* reveals new plant virus receptor candidates at the tip of maxillary stylets. J. Proteome Res. *19*, 1319–1337.

51. Guschinskaya, N., Ressnikoff, D., Arafah, K., Voisin, S., Bulet, P., Uzest, M., and Rahbé, Y. (2020). Insect mouthpart transcriptome unveils extension of cuticular protein repertoire and complex organization. iScience *23*, 100828.

52. Uzest, M., Gargani, D., Drucker, M., Hébrard, E., Garzo, E., Candresse, T., Fereres, A., and Blanc, S. (2007). A protein key to plant virus transmission at the tip of the insect vector stylet. Proc. Natl. Acad. Sci. USA *104*, 17959–17964.

53. Uzest, M., Gargani, D., Dombrovsky, A., Cazevieille, C., Cot, D., and Blanc, S. (2010). The "acrostyle": a newly described anatomical structure in aphid stylets. Arthropod Struct. Dev. *39*, 221–229.

54. Webster, C.G., Thillier, M., Pirolles, E., Cayrol, B., Blanc, S., and Uzest, M. (2017). Proteomic composition of the acrostyle: novel approaches to identify cuticular proteins involved in virus-insect interactions. Insect Sci. *24*, 990–1002.

55. Webster, C.G., Pichon, E., van Munster, M., Monsion, B., Deshoux, M., Gargani, D., Calevro, F., Jimenez, J., Moreno, A., Krenz, B., et al. (2018). Identification of plant virus receptor candidates in the stylets of their aphid vectors. J. Virol. *92*. e00432–18.

56. Chihota, C.M., Rennie, L.F., Kitching, R.P., and Mellor, P.S. (2001). Mechanical transmission of lumpy skin disease virus by *Aedes aegypti* (Diptera: Culicidae). Epidemiol. Infect. *126*, 317–321.

57. Chamberlain, R.W., and Sudia, W.D. (1961). Mechanism of transmission of viruses by mosquitoes. Annu. Rev. Entomol. *6*, 371–390.

58. Ramachandra Rao, T., Sharda Devi, P., and Singh, K.R.P. (1968). Experimental studies on the mechanical transmission of Chikungunya virus by *Aedes aegypti*. Mosquito News *28*, 406–408.

59. Boullis, A., Cordel, N., Herrmann-Storck, C., and Vega-Rúa, A. (2019). Experimental assessment of Zika virus mechanical transmission by *Aedes aegypti*. Viruses *11*, 695.

60. Colpitts, T.M., Cox, J., Vanlandingham, D.L., Feitosa, F.M., Cheng, G., Kurscheid, S., Wang, P., Krishnan, M.N., Higgs, S., and Fikrig, E. (2011). Alterations in the *Aedes aegypti* transcriptome during infection with West Nile, dengue and yellow fever viruses. PLoS Pathog. *7*, e1002189.

61. Dittmer, J., Alafndi, A., and Gabrieli, P. (2019). Fat body-specific vitellogenin expression regulates host-seeking behaviour in the mosquito *Aedes albopictus*. PLoS Biol. *17*, e3000238.

62. Untergasser, A., Cutcutache, I., Koressaar, T., Ye, J., Faircloth, B.C., Remm, M., and Rozen, S.G. (2012). Primer3—new capabilities and interfaces. Nucleic Acids Res. *40*, e115.

63. Altschul, S.F., Gish, W., Miller, W., Myers, E.W., and Lipman, D.J. (1990). Basic local alignment search tool. J. Mol. Biol. *215*, 403–410.

64. Di Tommaso, P., Moretti, S., Xenarios, I., Orobitg, M., Montanyola, A., Chang, J.M., Taly, J.F., and Notredame, C. (2011). T-Coffee: a web server for the multiple sequence alignment of protein and RNA sequences using structural information and homology extension. Nucleic Acids Res. *39*, W13–W17.

65. Fedorov, A., Beichel, R., Kalpathy-Cramer, J., Finet, J., Fillion-Robin, J.C., Pujol, S., Bauer, C., Jennings, D., Fennessy, F., Sonka, M., et al. (2012). 3D Slicer as an image computing platform for the quantitative imaging network. Magn. Reson. Imaging *30*, 1323–1341.

66. Nielsen, H., Engelbrecht, J., Brunak, S., and von Heijne, G. (1997). A neural network method for identification of prokaryotic and eukaryotic signal peptides and prediction of their cleavage sites. Int. J. Neural Syst. *8*, 581–599.

67. Gasteiger, E., Gattiker, A., Hoogland, C., Ivanyi, I., Appel, R.D., and Bairoch, A. (2003). ExPASy: the proteomics server for in-depth protein knowledge and analysis. Nucleic Acids Res. *31*, 3784–3788.

68. Louis-Jeune, C., Andrade-Navarro, M.A., and Perez-Iratxeta, C. (2012). Prediction of protein secondary structure from circular dichroism using theoretically derived spectra. Proteins *80*, 374–381.

69. Panjkovich, A., and Svergun, D.I. (2018). CHROMIXS: automatic and interactive analysis of chromatography-coupled small-angle X-ray scattering data. Bioinformatics *34*, 1944–1946.

70. Franke, D., Petoukhov, M.V., Konarev, P.V., Panjkovich, A., Tuukkanen, A., Mertens, H.D.T., Kikhney, A.G., Hajizadeh, N.R., Franklin, J.M., Jeffries, C.M., and Svergun, D.I. (2017). *ATSAS 2.8*: a comprehensive data analysis suite for small-angle scattering from macromolecular solutions. J. Appl. Crystallogr. *50*, 1212–1225.

71. Kabsch, W. (2010). Xds. Acta Crystallogr. D Biol. Crystallogr. *66*, 125–132.

72. Evans, P.R., and Murshudov, G.N. (2013). How good are my data and what is the resolution? Acta Crystallogr. D Biol. Crystallogr. *69*, 1204–1214.

73. Pape, T., and Schneider, T.R. (2004). HKL2MAP: a graphical user interface for macromolecular phasing with SHELX programs. J. Appl. Crystallogr. *37*, 843–844.

74. Sheldrick, G.M. (2010). Experimental phasing with SHELXC/D/E: combining chain tracing with density modification. Acta Crystallogr. D Biol. Crystallogr. *66*, 479–485.

75. Langer, G., Cohen, S.X., Lamzin, V.S., and Perrakis, A. (2008). Automated macromolecular model building for X-ray crystallography using ARP/wARP version 7. Nat. Protoc. *3*, 1171–1179.

76. Adams, P.D., Afonine, P.V., Bunkóczi, G., Chen, V.B., Davis, I.W., Echols, N., Headd, J.J., Hung, L.W., Kapral, G.J., Grosse-Kunstleve, R.W., et al. (2010). PHENIX: a comprehensive Python-based system for macromolecular structure solution. Acta Crystallogr. D Biol. Crystallogr. *66*, 213–221.

77. Emsley, P., Lohkamp, B., Scott, W.G., and Cowtan, K. (2010). Features and development of coot. Acta Crystallogr. D Biol. Crystallogr. *66*, 486–501.

78. Schneider, C.A., Rasband, W.S., and Eliceiri, K.W. (2012). NIH Image to ImageJ: 25 years of image analysis. Nat. Methods *9*, 671–675.

79. Di Venere, M., Fumagalli, M., Cafiso, A., De Marco, L., Epis, S., Plantard, O., Bardoni, A., Salvini, R., Viglio, S., Bazzocchi, C., et al. (2015). *Ixodes ricinus* and its endosymbiont *Midichloria mitochondrii*: a comparative proteomic analysis of salivary glands and ovaries. PLoS One *10*, e0138842.

80. Candiano, G., Bruschi, M., Musante, L., Santucci, L., Ghiggeri, G.M., Carnemolla, B., Orecchia, P., Zardi, L., and Righetti, P.G. (2004). Blue silver: a very sensitive colloidal Coomassie G-250 staining for proteome analysis. Electrophoresis *25*, 1327–1333.

81. Vandenborre, G., Smagghe, G., Ghesquière, B., Menschaert, G., Nagender Rao, R., Gevaert, K., and Van Damme, E.J. (2011). Diversity in protein glycosylation among insect species. PLoS One *6*, e16682.

82. Dzaki, N., and Azzam, G. (2018). Assessment of *Aedes albopictus* reference genes for quantitative PCR at different stages of development. PLoS One *13*, e0194664.

83. Schrödinger, L. (2010). The PyMOL molecular graphics system.

84. Studier, F.W. (2005). Protein production by auto-induction in high density shaking cultures. Protein Expr. Purif. *41*, 207–234.

85. Strub, M.P., Hoh, F., Sanchez, J.F., Strub, J.M., Böck, A., Aumelas, A., and Dumas, C. (2003). Selenomethionine and selenocysteine double labeling strategy for crystallographic phasing. Structure *11*, 1359–1367.

86. Pantoliano, M.W., Petrella, E.C., Kwasnoski, J.D., Lobanov, V.S., Myslik, J., Graf, E., Carver, T., Asel, E., Springer, B.A., Lane, P., and Salemme, F.R. (2001). High-density miniaturized thermal shift assays as a general strategy for drug discovery. J. Biomol. Screen. *6*, 429–440.

87. Hawe, A., Sutter, M., and Jiskoot, W. (2008). Extrinsic fluorescent dyes as tools for protein characterization. Pharm. Res. *25*, 1487–1499.

88. Bowler, M.W., Nurizzo, D., Barrett, R., Beteva, A., Bodin, M., Caserotto, H., Delagenière, S., Dobias, F., Flot, D., Giraud, T., et al. (2015). MASSIF-1: a beamline dedicated to the fully automatic characterization and data collection from crystals of biological macromolecules. J. Synchrotron Radiat. *22*, 1540–1547.

Please cite this article in press as: Arnoldi et al., A salivary factor binds a cuticular protein and modulates biting by inducing morphological changes in the mosquito labrum, Current Biology (2022), https://doi.org/10.1016/j.cub.2022.06.049

CellPress
OPEN ACCESS

STAR★METHODS

KEY RESOURCES TABLE

REAGENT or RESOURCE	SOURCE	IDENTIFIER
Antibodies		
αCp19#1	GeneScript Biotech	N/A
αCp19#2	GeneScript Biotech	N/A
αCp19#3	GeneScript Biotech	N/A
Goat anti-Rabbit IgG (H+L) Secondary Antibody, HRP	Thermo Fisher Scientific	Cat#32460; RRID: AB_1185567
GAL4 DNA-BD Monoclonal Antibody	Clontech	Cat#630403
Anti-GAL4 activation domain antibody produced in rabbit	Sigma-Aldrich	Cat#G9293; RRID:AB_439689
Goat anti-Mouse IgG (H+L) Secondary Antibody, HRP	Thermo Fisher Scientific	Cat#62-6520; RRID:AB_2533947
Goat anti-Rabbit IgG (H+L) Cross-Adsorbed Secondary Antibody, Texas Red-X	Thermo Fisher Scientific	Cat#T-6391; RRID:AB_2556779
Bacterial and virus strains		
Stellar Competent Cells, *E. coli* HST08 strain	Clontech	Cat#9128
T7 SHuffle *E. coli* K12 strain	New England Biolabs	Cat#C3026J
Biological samples		
Salivary Gland Extract from *Aedes albopictus* mosquitoes	This study	N/A
Saliva from *Aedes albopictus* mosquitoes	This study	N/A
Chemicals, peptides, and recombinant proteins		
Pilocarpine	Sigma-Aldrich	Cat#P6503; CAS: 54-71-7
Aureobasidin A	Clontech	Cat#630499
X-α-Gal	Clontech	Cat#630462
ProLong Diamond Antifade Mountant with DAPI	Thermo Fisher Scientific	Cat#P36962
ZYP-5052, Autoinduction Media	VWR Life Science	Cat#N990
In vitro synthetized peptide Cp19-C	ChinaPeptides	N/A
DCVJ	Sigma-Aldrich	Cat#72335; CAS: 58293-56-4
Drabkin's Reagent	Sigma-Aldrich	Cat#D5941
Brij L23 solution	Sigma-Aldrich	Cat#B4184, CAS: 9002-92-0
Selenomethionine	Sigma-Aldrich	Cat#1611955, CAS: 3211-76-5
albLIPS-2	This study	N/A
Cp19	This study	N/A
Cp19ΔC	This study	N/A
GFP-albLIPS-2	This study	N/A
GFP-albLIPS-2ΔHTH	This study	N/A
GFP-albLIPS-2(R38S)	This study	N/A
GFP-albLIPS-2(S151A; R152S)	This study	N/A
Critical commercial assays		
Pierce BCA Protein Assay Kit	Thermo Fisher Scientific	Cat#23225
Silver-Stain Plus kit	Biorad	Cat#1610449
PNGase-F	New England BioLabs	Cat#P0704S
PureLink RNA Mini Kit	Thermo Fisher Scientific	Cat#12183018A
SuperScript IV VILO Master Mix	Thermo Fisher Scientific	Cat#11756050
Invitrogen MEGAscript T7 Transcription Kit	Thermo Fisher Scientific	Cat#AM1334
Applied Biosystems SYBR Green PCR Master Mix	Thermo Fisher Scientific	Cat#4309155
QuantiFluor RNA System	Promega	Cat#E3310
LunaScript RT SuperMix Kit	New England BioLabs	Cat#E3010S

(*Continued on next page*)

Please cite this article in press as: Arnoldi et al., A salivary factor binds a cuticular protein and modulates biting by inducing morphological changes in the mosquito labrum, Current Biology (2022), https://doi.org/10.1016/j.cub.2022.06.049

Continued

REAGENT or RESOURCE	SOURCE	IDENTIFIER
Phusion High-Fidelity (HF) Polymerase Chain Reaction (PCR) with HF Buffer	New England BioLabs	Cat#M0531S
Wizard R SV Gel and PCR Clean-up System	Promega	Cat#A9281
In-Fusion HD Cloning Plus kit	Clontech	Cat#639650
Monarch Plasmid Miniprep Kit	New England Biolabs	Cat#T1010S
Make Your Own "Mate & Plate" Library System	Clontech	Cat#630490
Matchmaker Insert Check PCR Mix 2	Clontech	Cat#630497
Quick Ligation Mix	New England Biolabs	Cat#M2200S
Chitinase from *Streptomyces griseus* enzyme	Sigma-Aldrich	Cat#C6137
NEBuilder HiFi DNA Assembly Cloning Kit	New England Biolabs	Cat#E5520S
Deposited data		
Coordinates and structure factors	This study	PDB: 7TDS and 7TDR
SEC-SAXS experimental data	This study	SASBDB: SASDJX7
Sequences of clones	This study	N/A
Experimental models: Organisms/strains		
Aedes albopictus strain RIMINI	Department of Biology and Biotechnology (Università degli Studi di Pavia, Italy) and at the Department of Biosciences (Università degli Studi di Milano, Italy)	N/A
Saccaromyces cerevisiae yeast strains Y2Hgold	Clontech	Cat#630498
Saccaromyces cerevisiae yeast strains Y187	Clontech	Cat#630457
Oligonucleotides		
See Table S4	This study	N/A
Recombinant DNA		
pGBKT7	Clontech	Cat#630443
pGADT7 AD	Clontech	Cat#630442
pGADT7-Rec	Clontech	Cat#630490
Modified pET 28b	Department of Biology and Biotechnology (Università degli Studi di Pavia, Italy)	N/A
pBac{<af_attP-Ccb2t-tGFP_af<_PUb-DsRed} (#1260)	Department of Biology and Biotechnology (Università degli Studi di Pavia, Italy)[61]	N/A
Software and algorithms		
PD Quest version 8.0.1 software	Bio-Rad	https://pdquest.software.informer.com/8.0/
Xcalibur software 1.4	Thermo Fisher Scientific	https://www.thermofisher.com/order/catalog/product/OPTON-30965
Peaks studio 4.5 software	Bionformatics Solutions	https://www.bioinfor.com/download-peaks-studio/
Primer3Plus	Untergasser et al.[62]	https://www.primer3plus.com/
MAESTRO software	Bio-Rad	https://www.bio-rad.com/it-it/product/cfx-maestro-software-for-cfx-real-time-pcr-instruments?ID=OKZP7E15
Basic Local Alignment Search Tool (BLAST)	Altschul et al.[63]	https://blast.ncbi.nlm.nih.gov/Blast.cgi
T-COFFEE	Di Tommaso et al.[64]	https://tcoffee.crg.eu/
PyMOL software	Schrodinger	https://pymol.org/2/
Slicer 3D software	Fedorov et al.[65]	https://www.slicer.org/
SignalP-6.0	Nielsen et al.[66]	https://services.healthtech.dtu.dk/service.php?SignalP
Expasy ProtParam tool	Gasteiger et al.[67]	https://web.expasy.org/protparam/

(*Continued on next page*)

Continued

REAGENT or RESOURCE	SOURCE	IDENTIFIER
Olympus OLS400 3.1.9 software	Olympus	=https://www.olympus-ims.com/en/service-and-support/downloads/#!dlOpen=%2Fen%2Fdownloads%2Fdetail%2F%3F0%5Bdownloads%5D%5Bid%5D%3D276827017
K2D3 software	Louis-Jeune et al.[68]	http://cbdm-01.zdv.uni-mainz.de/~andrade/k2d3/
CHROMIXS	Panjkovich and Svergun[69]	https://www.embl-hamburg.de/biosaxs/chromixs.html
ATSAS	Franke et al.[70]	https://www.embl-hamburg.de/biosaxs/download.html
XDS	Kabsch[71]	https://xds.mr.mpg.de/html_doc/downloading.html
Aimless	Evans and Murshudov [72]	https://www.ccp4.ac.uk/html/aimless.html
HKL2MAP	Pape and Schneider[73]	http://webapps.embl-hamburg.de/bundle/download.php?hkl2mp=true&sitcom=false
SHELXC/D	Sheldrick[74]	https://strucbio.biologie.uni-konstanz.de/ccp4wiki/index.php/SHELX_C/D/E
SHELXE	Sheldrick[74]	https://www.shelxle.org/shelx/eingabe.php
ARP/wARP	Langer et al.[75]	http://www.embl-hamburg.de/ARP/
Phenix	Adams et al.[76]	https://phenix-online.org/download
Coot	Emsley et al.[77]	https://www.mrc-lmb.cam.ac.uk/personal/pemsley/coot/binaries/
MO.Control software (v1.6)	Nanotemper	https://nanotempertech.com/monolith-mo-control-software/
MO.Affinity (v2.2)	Nanotemper	https://nanotempertech.com/monolith/
ImageJ	Schneider et al.[78]	https://imagej.nih.gov/ij/
Prism9-GraphPad	Dotmatics	https://www.graphpad.com
Other		
VersaDoc 3000 Microplate Reader	Bio-Rad	http://www.medwow.com/med/microplate-reader/bio-rad-laboratories/versadoc-3000/70931.model-spec
Jupiter C18	Phenomenex	http://hplcmart.com/hplc/viewproduct/id:11114/jupiter-c18/phenomenex/reversed-phase#undefined
Linear Trap Quadrupole (LTQ) mass spectrometer with electrospray ionization ion source	Thermo Fisher Scientific	https://www.thermofisher.com/order/catalog/product/IQLAAEGAAVFACZMAIK?SID=srch-srp-IQLAAEGAAVFACZMAIK
Nanoject II Auto-Nanoliter Injector	Drummond	https://www.drummondsci.com/product/microinjection/nanoject-ii-auto-nanoliter-injector/
A1/A1R confocal microscope	Nikon	https://www.nikon.com/news/2018/0830_a1_a1r_01.htm
Äkta purifier	GE Healthcare	Cat# GE29-0220-94
Olympus LEXT OLS4100 3D Measuring Laser Microscope	Olympus	https://www.olympus-ims.com/en/metrology/ols4100/
MiniOpticon real-time PCR detection system	Bio-Rad	N/A
Tycho NT.6	Nanotemper	N/A
Jasco J-700 spectropolarimeter	Jasco-Europe, Cremella, Italy	https://jascoinc.com/products/spectroscopy/circular-dichroism/j-1000-series-models/j-1700-circular-dichroism-spectrophotometer/
Nexera High Pressure Liquid/Chromatography	Shimadzu	https://www.shimadzu.com/an/products/liquid-chromatography/hplcuhplc/nexera-series/index.html
Oryx 8	Douglas Instruments	https://www.douglas.co.uk/oryx8.htm

(*Continued on next page*)

Please cite this article in press as: Arnoldi et al., A salivary factor binds a cuticular protein and modulates biting by inducing morphological changes in the mosquito labrum, Current Biology (2022), https://doi.org/10.1016/j.cub.2022.06.049

Continued

REAGENT or RESOURCE	SOURCE	IDENTIFIER
Monolith NT.115 instrument	Nanotemper	https://nanotempertech.com/monolith/monolith-nt115/
HisTrap excel column	Cytiva	Cat#17371206
Superdex 75 10/300 GL column	Cytiva	Cat#17517401
HiTrap Capto Q ImpRes anion exchange column<	Cytiva	Cat#17547051
HiPrep 26/10 Desalting column	Cytiva	Cat# 17508702

RESOURCE AVAILABILITY

Lead contact

Further information and requests for resources and reagents should be directed to and will be fulfilled by the lead contact, Paolo Gabrieli (paolo.gabrieli@unimi.it).

Materials availability

Primary antibodies against Cp19 are available upon request to the lead contact.

Data and code availability

- Coordinates and structure factors have been deposited at Protein Data Bank (PDB) and are publicly available as of the date of publication. Accession numbers are listed in the key resources table.
- SEC-SAXS experimental data have been deposited at Small Angle Scattering Biological Data Bank (SASBDB) and are publicly available as of the date of publication. Accession numbers are listed in the key resources table.
- This paper does not report original code.
- Any additional information required to reanalyze the data reported in this paper is available from the lead contact upon request.

EXPERIMENTAL MODEL AND SUBJECT DETAILS

- *Aedes albopictus* were collected from the "RIMINI" breeding colony at the Department of Biology and Biotechnology (Università degli Studi di Pavia, Italy) and at the Department of Biosciences (Università degli Studi di Milano, Italy), and reared as previously reported.[61]
- The protocol for acquiring data on mosquito biting behavior on human subjects has been approved by the Ethical Committee of the University of Milan (13.22).
- For proteins expression and purification, T7 SHuffle *E. coli* K12 strain (New England Biolabs) were grown in ZYP-5052 auto-inducing medium at 30°C for 4.5 hours and 20°C over night.
- For yeast two hybrid screening assays, the *Saccaromyces cerevisiae* yeast strains Y2Hgold (genotype: MATa, trp1-901, leu2-3, 112, ura3-52, his3-200, gal4Δ, gal80Δ, LYS2 : : GAL1UAS–Gal1TATA–His3, GAL2UAS–Gal2TATA–Ade2 URA3 : : MEL1UAS–Mel1TATA AUR1-C MEL1) and Y187 (genotype: MATα, ura3-52, his3-200, ade2-101, trp1-901, leu2-3, 112, gal4Δ, gal80Δ, met-, URA3 : : GAL1UAS–Gal1TATA–LacZ, MEL1) were grown on sterile YPDA (Yeast extract Peptone Dextrose supplemented with Adenine hemisulfate) or appropriate minimal medium to maintain plasmids at 30°C.

METHOD DETAILS

Insect rearing

Aedes albopictus were collected from the "RIMINI" breeding colony at the Department of Biology and Biotechnology (Università degli Studi di Pavia, Italy) and at the Department of Biosciences (Università degli Studi di Milano, Italy). This strain was established in 2004 from mosquitoes collected in Rimini, Italy and maintained under standard insectary conditions (27 ± 1 °C, 65–80% relative humidity, 12:12 h light/dark photoperiod). Larvae were fed daily with carp fish pellets (Tetramin, Tetra) till pupation. Pupae were collected in a small cup of water and moved to a mosquito cage (Bugdorm). Adults were maintained on a 10% sucrose solution provided *ad libitum* and the females blood-fed on animal blood using *in vitro* system.

Sample preparation for proteomics analysis

For saliva collection, mature, 6-7 days old female mosquitoes (200 each biological replicate for five replicates) were cold-anesthetized, legs and wings removed, and the proboscis inserted in a plastic micro-pipette tip containing 1 μL of PBS. Salivation was

Please cite this article in press as: Arnoldi et al., A salivary factor binds a cuticular protein and modulates biting by inducing morphological changes in the mosquito labrum, Current Biology (2022), https://doi.org/10.1016/j.cub.2022.06.049

induced by topical application of 1% (w/v) Pilocarpine (PBS + 0.2% Tween-20). After 45 minutes the mosquitoes were removed and the PBS solution from the tips collected, concentrated using speed-vacuum and protein concentration was measured using the Bicinchoninic Acid (BCA) assay (Pierce). The volume was adjusted to 100 μL with the addition of Ammonium bicarbonate (100 mM, pH 7.4) and sequencing grade trypsin (20 ng/μl Promega) and incubated at 37 °C overnight. The digested mixture was then lyophilized and stored at -80 °C till mass spectrometric analysis. In preliminary experiments aimed at assessing the quality of the recovered proteins, these have been analyzed through SDS-PAGE and stained using silver-staining (Bio-Rad) following the manufacturer's protocol.

For salivary gland extracts, 60 female mosquitoes per replicate (either in the first 24 hours after emergence or 6 days old) were cold-anesthetized and the salivary glands dissected in PBS using fine forceps under a stereomicroscope. Salivary glands were collected in 100 μL of PBS, extracted using a polypropylene pestle and centrifuged in a microcentrifuge for 20 min at 4 °C at maximum speed. The mild extraction was performed in order to not solubilize the membranes of the salivary gland cells and to collect mostly the extracellular secreted fraction. Protein content of the extracts was quantified using the BCA assay and the extracts were dried using speed-vacuum. Proteins were dissolved in 125 μL of rehydration buffer (8 M urea, 4% CHAPS (w/v), 65 mM Dithioerythritol, 0.8% carrier ampholytes (v/v), 0.5% bromophenol blue) and analyzed using a Two-Dimensional Gel Electrophoresis (2-DE) as previously described.[79] Briefly, proteins were first loaded onto 7 cm immobilized pH gradient (IPG)strips, with nonlinear (NL) pH 3–10 gradient range (Amersham Biosciences) in an Ettan IPGphor system (Amersham Biosciences) at 15 °C, with the following voltage gradient: 30 V for 8 h, 120 V for 1 h, 500 V for 0.5 h, 1000 V for 0.5 h and 5000 V until a total of 25–27 kV/h was reached. The focused IPG strips were reduced, alkylated and SDS PAGE was performed in a PROTEAN II xi 2-D Cell equipment (Bio-Rad) with a 10 mA current per gel. "Blue silver" was used to visualize the 2-DE gels.[80] Stained gels were scanned using VersaDoc Imaging Model 3000 (Bio-Rad) and the digital images were analyzed using PD Quest (Bio-Rad) version 8.0.1 software. Enzymatic digestion and peptide extraction were then performed as previously reported.[79] Excised spots were first de-stained using 100 mM ammonium bicarbonate buffer pH 7.8, 50% acetonitrile (ACN), dehydrated in ACN and reduced in 10 mM DTT. After the addition of iodoacetamide and extensive washes, proteins spots in the gel pieces were digested with sequencing-grade trypsin (20 ng/μl in 100mM ammonium bicarbonate, pH 7.8) and the tryptic peptides extracted with three washes: 50% ACN, 5% trifluoroacetic acid (TFA) and 100% ACN. The washes were pooled, dried and stored at -80 °C till mass spectrometry analyses.

LC-MS/MS Analysis

Tryptic peptides were separated on a C18 column by RP-HPLC on a Jupiter (Phenomenex, Torrance, CA, USA) at 0.2 mL/min using a linear gradient of ACN in 0,1% Formic Acid (FA). 2–60% solvent B in 60 min) in which solvent A consisted of 0.1% aqueous FA and solvent B consisted of ACN containing 0.1% FA. Separated peptides were analyzed in a Linear Trap Quadrupole (LTQ) mass spectrometer with electrospray ionization ion source controlled by Xcalibur software 1.4 and the generated data were studied using Peaks studio 4.5 software. An *ad-hoc* database was generated using genes predicted from published genomes as reference.

Deglycosylation assay

Being all the salivary proteins secreted, we expect that they might be glycosylated. As the majority of glycosylation is N-glycan in the majority of insect species analyzed,[81] we treated extracts with recombinant PNGase-F (New England BioLabs). Briefly, Glycoprotein Denaturing Buffer (New England BioLabs) was added to protein extracts to reach a 1X concentration and the proteins were denatured at 95 °C for 10 minutes. After cooling, glycobuffer 2 (New England BioLabs), 1% NP-40, and 0.2 μL (100 Units) of recombinant PNGase F were added and incubated at 37°C for 2 hours. The protein mixture was then analyzed using 2-DE, as previously described.

In vivo RNA-interference (RNAi)

The transient knockdown of the expression of *LIPS-2* gene was achieved by injecting long dsRNA in adult females.[36] Briefly, RNA was extracted from 60 pairs of salivary glands dissected in PBS from mature adult *Ae. albopictus* females using the RNA PureLink Mini Kit (Invitrogen, Carlsbad, CA, USA) and treated with DNAse. Subsequently, cDNA was synthesized using SuperScript IV VILO (Invitrogen) from 100 ng of total RNA following the manufacturer's instructions. The synthetized cDNA was then used to amplify a 701 bp cDNA fragment of *LIPS-2* using primers containing the T7 promoter sequence (T7-LIPS2fw and T7-LIPS2rv; see Table S4), designed using Primer3Plus[62] and the following this cycling program: 95 °C for 2 min, 10 cycles of 95 °C for 10 seconds and 59 °C for 30 seconds and 72°C for 30sec, 25 cycles of 95 °C for 10 seconds and 72 °C for 45 seconds. Similarly a fragment of the *turbo green fluorescent protein* gene was amplified from the pBac{<af_attP-Ccb2t-tGFP_af<_PUb-DsRed} (#1260) plasmid using the primers T7-GFPfw and T7-GFPrv (see Table S4)[61] to generate dsGFP as control. After purification with Wizard R SV Gel and PCR Clean-up System (Promega), 200 ng of each PCR product (in 2 μl) were used as template to generate dsRNAs using the T7 Megascript kit (Ambion) and following the manufacturer's protocol. Newly emerged females (<24 h of age) were cold-anesthetized and injected in the thorax with 138 nL of dsRNA for both dsLIPS-2 or dsGFP using NanojectII (Drummond), injecting about 1 μg of dsRNA/mosquito. Mosquitoes were transferred in cups for recovery and kept in the insectary with a solution of 20% sucrose till behavioral testing or dissection.

Gene expression analysis by RT-qPCR

The *LIPS-2* expression levels were verified using RT-qPCR in RNA extracted from dsRNA-injected females (either dsLIPS-2 or dsGFP) after 3 days from the injection. RNA was extracted from pools of five thoraxes and cDNA was synthetized as described in

the previous section. A total of 4 biological replicates for both the experimental and control group were generated. For qPCR, 15 μL reactions were set up in duplicates using 1× Power SYBR Green Master Mix (Applied Biosystems) on the CFX Connect Real-Time System (Bio-Rad) using the following cycles: 95°C for 10 min, followed by 40 cycles of 95°C for 10 seconds and 55°C for 30 seconds, followed by a melt curve. Gene expression was normalized using the deltaCT method against the Ribosomal Protein S17 as a housekeeping gene and *LIPS-2* gene specific primers (qRPS17fw and qRPS17rv;[82] qLIPS-2fw and qLIPS-2rv; see also Table S4). Differences in *LIPS-2* gene expression between dsLIPS-2 and dsGFP injected females were tested using the MAESTRO software (Bio-Rad).

To evaluate the *Cp19* expression during labrum development, *Ae. albopictus* female pupae were collected 0, 4, 8, 24 and 48 hours after the beginning of the pupation process. Samples were dried and stored at -80°C until processing. Labra were dissected in PBS and crushed with a pestle in lysis buffer (Pure Link RNA Mini Kit, Thermo Fisher Scientific) supplemented with β-mercaptoethanol. RNA was extracted following manufacturer's instructions, quantified (QuantiFluor RNA System, Promega) and retrotranscribed (LunaScript RT SuperMix Kit, New England Biolabs) following manufacturer's instructions. The reaction mixture was incubated at 25 °C for 5 min, 55 °C for 20 min and 95 °C for 1 min. The expression of the cuticular protein Cp19 was assessed using the specific primers qCp19fw, and qCp19rv (see also Table S4) using the same program as described for LIPS-2.

Behavioral assay

3 days after injection, 20% sucrose solution was removed from cages 2-3 hours before the start of the experiment. Mosquitoes were tested for their blood-feeding behavior: each single mosquito was placed in a cage in which the arm of a volunteer was inserted in the cage. The cages have a transparent side to allow easy observation. When the mosquito approached the arm and started inserting the proboscis for feeding, the operators measured the time each mosquito took to 1) reach a blood vessel and start feeding (intradermal probing) 2) time to complete the feeding (feeding time). The period of the intradermal probing was calculated as the time occurring between the insertion of the proboscis into the skin and the beginning of the feeding, as visible by the blood starting filling the gut, while the feeding time started from this point till the mosquito detached from the biting site.

Soon after feeding, mosquitoes were cold-anesthetized, and abdomens separated from the rest of the body and used to quantify the hemoglobin content using a colorimetric assay and Drabkin's Reagent (Sigma-Aldrich). Abdomens were homogenized in 1 mL Drabkin's reagent supplemented with Brij 23 solution (Sigma-Aldrich) and then cleared in a microcentrifuge for 20 minutes at maximum speed. A standard curve was prepared using known concentrations of haemoglobin and absorbance of the samples were read at 540 nm in a spectrophotometer.

Data from the probing and feeding time were Log_{10} transformed to achieve normality and differences between the two groups tested by unpaired t tests. p values were FDR corrected to avoid statistical type I error for multiple testing.

Yeast two-hybrid screening

Cloning and testing bait for autoactivation

LIPS-2 CDS was amplified using Phusion High-Fidelity (HF) Polymerase Chain Reaction (PCR) with HF Buffer (New England Biolabs) (5 min denaturation at 95 °C, 15 cycles of denaturation at 95 °C for 10 s, annealing at 55 °C for 30 s, and elongation at 72 °C for 30 s and 25 cycles of denaturation at 95 °C for 10 s, and annealing/elongation at 72 °C for 30 s and a final elongation step of 5 min at 72 °C). Primers were specifically designed to allow the *in vitro* cloning into linearized pGBKT7 vector (pGBKT7-LIPS-2fw and pGBKT7-LIPS-2rv; see also Table S4) previously linearized by digestion with EcoRI and BamHI restriction enzymes for 2 hours at 37 °C. The pGBKT7 vector and the insert were purified (Wizard R SV Gel and PCR Clean-up System, Promega) and quantified using a Qubit fluorometer (Qubit dsDNA HS Assay Kit, Thermo Fisher Scientific). Cloning of LIPS-2 sequence was performed according to the manufacturer's instructions (In-Fusion HD Cloning Plus kit). Briefly, the reaction mixture was incubated at 50 °C for 15 minutes. Then, Stellar Competent Cells (SCCs) were transformed with 2.5 μL of the In-Fusion reaction mixture and incubated at 4 °C for 30 minutes. Afterwards, SCCs were heat-shocked at 42 °C for 45 seconds, cooled in ice and incubated shaking in pre-warmed Super Optimal broth with Catabolite repression (SOC) medium at 37 °C for 1 hour. Transformants were selected by growth on Lysogeny Broth (LB) agar plates supplemented with kanamycin (Kan) 50 μg/mL for 24 hours at 37°C. Plasmid DNA was isolated using standard methods (Monarch Plasmid Miniprep Kit, New England Biolabs) and sequenced using the T7 standard primer (Eurofins Genomics, Ebersberg, Germany).

Y2HGold yeast strain was transformed with pGBKT7-LIPS-2 plasmid (i.e., Y2HGoldLIPS-2) following small-scale transformation protocol (Yeastmaker Yeast Transformation System 2 User Manual). Briefly, cells were grown in YPDA broth until reaching the suitable Optical Density (OD) 600. After a wash in distilled water (dH2O), cells were resuspended in Tris-EDTA (TE)/Lithium Acetate (LiAc) buffer. The plasmid (100 ng), the denatured Yeastmaker carrier DNA, PEG/LiAc buffer and 50 μL of the competent cells were combined into a pre-chilled tube and incubated at 30 °C for 30 minutes. Subsequently, DMSO was added to the mixture and the tube was placed at 42 °C for 15 minutes. Cells were collected by centrifugation, resuspended in YPD Plus Medium and incubated at 30 °C for 1 hour. The cell pellet was resuspended in NaCl 0.9% and plated on minimal medium Single Dropout (SDO)/-Tryptophan (Trp) agar plates for 3 days at 30 °C. To exclude the autoactivation of GAL4 promoter by the GAL4 BD-LIPS-2 fusion protein, Y2HGold-LIPS-2 was grown in the same conditions on the same medium supplemented with the antibiotic Aureobasidin A (AuA, 200 ng/mL).

Custom-made labrum cDNA library generation

Labra were dissected in Phosphate Buffer Saline (PBS) under a stereomicroscope (Leica M50) from *Ae. albopictus* female pupae (70 individuals between 0 and 24 hours after pupation and 30 individuals older than 24 hours) and RNA was extracted as previously described. The custom-made labrum cDNA library was generated following the Make Your Own "Mate & Plate" Library System

User Manual. First strand cDNA was synthetized from extracted RNA using the oligo-dT (CDSIII) primer and the SMART III-modified oligo (SMART technology). Double strand cDNA was synthetized by Long Distance PCR (LD-PCR) and purified using CHROMA SPIN+TE-400 Columns, for selection of DNA molecules longer than 200 bp. The library-scale transformation of competent Y187 strain cells, which allowed the *in vivo* recombination of dscDNA into pGADT7-Rec vector, was performed following the Yeastmaker Yeast Transformation System 2 User Manual. Briefly, the cDNA, the vector, the Yeastmaker Carrier DNA, 2.5 mL of PEG/LiAc and 600 μL of competent cells were assembled into a pre-chilled tube and processed as described above, with minor modifications. The mixture was plated on SDO/- Leucine (Leu) minimal medium and incubated at 30 °C for selection of transformants. After 3 days, agar plates were placed at 4 °C to stop the growth of yeasts and the colonies were harvested in freezing medium (10 mL YPDA, 3.5 mL glycerol, 1.5 mL dH2O) and pooled together in a single sterile flask. Cells were counted using a hemocytometer and the solution was aliquoted into several single-use vials which were stored at -80 °C until usage.

Yeast two-hybrid (YTH) assay

The custom-made labrum cDNA library was screened for interaction with the bait protein LIPS-2 according to Matchmaker Gold Yeast Two-Hybrid System User Manual guidelines. In brief, Y2HGoldLIPS-2 was inoculated in SDO/-Trp broth and incubated shaking at 30 °C until the OD_{600} reached 0.8 units. Cells were centrifuged and combined with one aliquot of the custom-made labrum cDNA library. The library was titrated by plating serial dilutions (1:10, 1:100, 1:1000, 1:10000) on SDO/-Leu agar plates. Mating was carried out in 2X YPDA broth supplemented with Kan 50 μg/mL. The mating solution was assessed for the presence of zygotes under an optical microscope (40X, Leica DM1000) after 20 hours of incubation at 30 °C under constant slow agitation and then processed following the manufacturer's instructions. The final pellet was resuspended in 0.5X YPDA added with Kan 50 μg /mL and the total volume of the solution was measured. The culture was titrated by plating serial dilutions on SDO/-Trp, SDO/-Leu and Double Dropout (DDO)/-Leu/-Trp agar plates to evaluate the mating efficiency, calculated as the ratio between the viability, or rather the number of colony forming unit (cfu)/mL, of diploids and that of the limiting partner (i.e., the strain with the lower viability). Interactors were selected by plating the remainder of the culture on DDO/-Leu/-Trp agar plates supplemented with AuA (200 ng/mL) and X-α-gal (40 μg/mL). Agar plates were incubated at 30 °C for 3 days. Interactors were stripped on Quadruple Dropout (QDO)/-Leu/-Trp/-Adenine (Ade)/-Histidine (His) agar plates supplemented with AuA (200 ng/mL) and X-α-gal (4 mg/mL) and incubated at 30 °C for 3 days for additional selection.

The prey plasmids hypothetically coding for interacting proteins were amplified by Matchmaker Insert Check PCR. Briefly, yeast colonies were selected from QDO agar plates and each one was dissolved into sterile dH2O. An equal volume of the Insert Check PCR Mix 2 was added and the amplification was carried out under the following thermal cycling conditions: 1 min denaturation at 94 °C, 30 cycles of denaturation at 98 °C for 10 s, annealing/elongation at 68 °C for 3 min and a final elongation step of 10 min at 68 °C. PCR products were visualized on a 1% agarose gel, grouped on the basis of their apparent molecular weight and selected for sequencing with the standard T7 primer. Sequences were identified using nucleotide Basic Local Alignment Search Tool (BLAST)[63] against the non-redundant nucleotide database of the National Center for Biotechnology Information (NCBI).

Primers targeting the C-terminal portion of *Ae. albopictus* Cp19-like protein (Cp19pep) transcript (LOC109403106) (Cp19pepfw and Cp19peprv; see also Table S4) were used to screen back the prey cDNAs by PCR.

Co-transformation and autoactivation assays

Cp19pep sequence was amplified by Matchmaker Insert Check PCR and cloned *in vitro* into pGADT7-Rec vector (pGADT7-Rec-Cp19pep). Cp19 full length transcript was amplified by PCR on first strand cDNA which had been synthetized for the generation of the custom-made labrum cDNA library. Primers were designed to allow the *in vitro* cloning into linearized pGADT7 (pGADT7-Cp19flfw and pGADT7-Cp19flrv; Table S4) or pGBKT7 vectors (pGBKT7-Cp19flfw and pGBKT7-Cp19flrv; Table S4). pGADT7 was linearized as previously described for pGBKT7 vector. *In vitro* cloning was performed as depicted above. LIPS-2 PCR product was digested with EcoRI and BamHI restriction enzymes and ligated into linearized pGADT7 vector (pGADT7-LIPS-2) according to manufacturer's instructions (Quick Ligation Mix, New England Biolabs).

Y2HGold yeast strain was transformed with pGADT7, pGBKT7, pGADT7-Cp19pep, pGADT7-Cp19fl, pGADT7-LIPS-2, pGBKT7-Cp19fl (100 ng/each) and plated on SDO/-Leu (for pGADT7-) or SDO/-Trp (for pGBKT7-) supplemented or not with AuA (200 ng/mL) and X-α-gal (4 mg/mL) to exclude autoactivation of GAL4 promoter.

Moreover, the yeast strain was co-transformed with pGBKT7-LIPS-2 and pGADT7-Cp19pep or pGBKT7-LIPS-2 and pGADT7-Cp19fl or pGBKT7-Cp19fl and pGADT7-LIPS-2 plasmids (100 ng/each) and plated on DDO/-Leu/-Trp supplemented or not with AuA (200 ng/mL) and X-α-gal (4 mg/mL) to confirm interaction between bait and prey proteins. Co-transformations were performed following Yeast Protocols Handbook guidelines (Takara).

RANDOM MUTAGENESIS OF LIPS-2 COUPLED TO Y2H

Random mutagenesis of LIPS-2 transcript was performed by error-prone (ep) PCR.[47] The epPCR reaction mixture (50 μL) contained 10 mM Tris– HCl pH 8.4, 50 mM KCl, 7 mM MgCl2, 5 mM MnCl2, biased nucleotide composition (1 mM each of dCTP and dTTP, 0.2 mM each of dATP and dGTP), 500 nM each of the oligonucleotide primers (LIPS-2fw, LIPS-2rv), 1% dimethyl sulfoxide (DMSO), 1.6 U GoTaq DNA Polymerase (Promega) and 1 pg of DNA template. PCR conditions were those described above for the corresponding primers. PCR product was checked on an agarose gel 1.2% m/v, purified and cloned *in vitro* into linearized pGBKT7 vector.

Y187 strain competent cells were prepared and transformed following the manufacturer's instructions with minor modifications of the small-scale transformation protocol. The library was screened for interaction with Cp19fl protein, expressed by YTHGoldCp19fl yeast clone, in a YTH assay, as previously described. LIPS-2 sequence was amplified by colony-PCR on clones growing on selective medium. PCR products were purified, sequenced, and aligned to LIPS-2 transcript using T-COFFEE.[64] Point mutations were visualized on the model of the 3D protein structure using PyMOL software.[83]

Western blot analysis

To assess the expression of proteins in yeasts, yeast protein extracts were obtained by all transformed and co-transformed yeasts following the Urea/SDS Extraction Method described in Yeast Protocols Handbook with minor modifications. Briefly, cultures were centrifuged, and pellets were resuspended in pre-warmed cracking buffer (Tris-HCl pH 6.8 40 mM, Urea 8 M, SDS 5% w/v, EDTA 0.1 mM) supplemented with β-mercaptoethanol 0,9% v/v and phenylmethylsulphonyl fluoride (PMSF), which was added twice according to manufacturer's suggested concentration to overcome protein degradation. Vigorous vortexing instead of usage of glass beads was employed to break cells. Soluble fractions were collected by centrifugation and used for western blot analysis.

To assess the expression of Cp19 protein in adult mosquitoes, 6 days-old females mosquitoes were collected and cold-anesthetized. Labra were dissected and pooled in groups of 5, 10 and 20 stylets. Samples were incubated at room temperature for 1, 2, 4 hours or overnight with Chitinase from *Streptomyces griseus* enzyme (2 U/mL, Sigma-Aldrich) supplemented with $CaCl_2$ (2 mM) and subjected to high-speed centrifugation. Supernatants and pellets were resuspended in loading buffer added with dithiothreitol (DTT), boiled, and stored at -20 °C until usage.

Samples were separated by SDS-PAGE gel, followed by electrophoretic transfer to a polyvinylidene fluoride membrane, which was blocked and incubated with the primary antibodies. The following antibodies were used in these experiments: the monoclonal antibody αCp19#3 (1:1000); the Goat anti-Rabbit IgG (H+L) Secondary Antibody, HRP (1:30000) (Thermo Fisher Scientific), the GAL4 DNA-BD Monoclonal Antibody (0.5 μg/ml), the Anti-GAL4 activation domain antibody produced in rabbit (0,5 ug/mL, Sigma-Aldrich) and the Goat anti-Mouse IgG (H+L) Secondary Antibody, HRP (Thermo Fisher Scientific).

Immunofluorescence assays

Rabbit monoclonal antibodies against Cp19 (epitope #1: DGHTHDHKSQWEHR; epitope #2: DEADGTHRIVDYSS; epitope #3: RVGHAHHPHGESYA) and a control rabbit IgG antibody were synthetized by GeneScript Biotech (Leiden, Netherlands). To assess the presence and the localization of the cuticular protein on the mosquito labrum, mature female mosquitoes (> 6 days-old) were cold-anesthetized and the head was separated by the rest of the body; the antennae and the labium were removed using a pair of forceps. Heads were incubated overnight at 4 °C with each anti-Cp19 antibody or with the control antibody at the manufacturer's supplied concentration (αCp19#1: 0.609 mg/mL, αCp19#2: 0.988 mg/mL, αCp19#3: 1.553 mg/mL). After washes in PBS-Tween 20 (PBST; Fisher BioReagents) 0.1% v/v and incubation with Texas-Red-X goat anti-rabbit IgG (H+L) 1:200 (Molecular Probes, Thermo Fisher Scientific) for 3 hours at 4 °C, the labrum was separated from the other stylets and incubated with Green Fluorescent Protein GFP-albLIPS-2 (2 mg/mL). Fluorescence was visualized under the Carl Zeiss Axiovert 200M Motorized Inverted Microscope. Images were captured using the Carl Zeiss Camera Microscope AxioCam MRM (Thermo Fisher Scientific).

In the case of αCp19#3, samples were observed at the confocal microscope (Unitech NOLIMITS platform, Unimi).

For confocal microscopy analysis, newly emerged female mosquitoes (less than 12-hours old) were collected and cold-anesthetized. Labra were dissected, mounted on a microscope slice in ProLongTM Diamond Antifade Mountant with DAPI (Thermo Fisher Scientific) and stored at 4 °C in the dark until the observation at the single-photon confocal microscope (Unitech NOLIMITS platform, Unimi). Fluorescence was visualized at a 60X magnification. The 3D organization of cellular nuclei at the tip of the labrum was reconstructed using the Slicer 3D software.[65]

Protein expression and purification

The LIPS-2 coding sequence from *Aedes albopictus* (GenBank: mRNA AY826118.1, protein AAV90690,; UniProt: Q5MIU2) deprived of the region encoding for the signal peptide (residues 1-25, as predicted using SignalP software)[66] was amplified from salivary glands cDNA using the primers pET28b - LIPS-2fw, pET28b - LIPS-2rv, GFP-LIPS-2fw, GFP-LIPS-2rv_Nterm (Table S4). The Cp19 coding sequence from *Aedes albopictus* (mRNA XM_019675843) deprived of the region encoding for the signal peptide (residues 1-17, as predicted using SignalP software) was amplified from the genomic DNA using the primers pET28b Cp19flfw, pET28b Cp19flrv and pET28b-Cp19ΔCrv (Table S4). The amplicons were subcloned into a modified pETSUMO vector (Invitrogen), which allows for the expression of recombinant proteins fused at their N-terminus to a 8xHis-tag followed by the SUMO protein, or into a modified pET28b vector allowing expression of recombinant proteins fused at the N-terminus with a 8xHis-tag followed by green fluorescent protein (GFP). The recombinant proteins were expressed in the T7 SHuffle *E. coli* K12 strain (New England Biolabs) using ZYP-5052 autoinducing medium.[84] After inoculation, cells were grown at 30°C for 4.5 hours and then overnight at 20°C. Selenomethione (SeMet) labeling of albLIPS-2 was obtained through metabolic inhibition of the bacterial synthesis of the endogenous methionine, forcing the inclusion of the SeMet provided in the broth.[85] Briefly, an overnight pre-culture in LB of the T7 SHuffle *E. coli* K12 cells transformed with the pET-albLIPS-2 plasmid was re-inoculated in M9 minimal medium supplemented with 100 mg/L of each branched amino acid and grown at 30 °C. When the OD_{600} reached 0.3, 100 mg/L of each amino acid inhibiting the methionine synthesis were added (Lysine, Phenylalanine, Threonine, Proline) together with 50 mg/L of SeMet. After 15 min, protein expression was induced with 0.5 mM IPTG and the cells were then grown overnight at 20 °C.

Harvested cells were resuspended in buffer A (25 mM HEPES/NaOH, 500 mM NaCl, pH 8.0) and lysed by sonication. After clearance by centrifugation at 75'000 *g* for 45 minutes at 4°C, recombinant proteins were purified at room temperature using liquid chromatography (Äkta purifier, GE Healthcare) through immobilized metal ion affinity chromatography (IMAC) using a 5 ml HisTrap excel column (Cytiva), followed by removal of the purification tag by incubating the IMAC elution with His-tagged SUMO protease in dialysis in buffer A at 4°C overnight. Removal of the cleaved His-SUMO tag and His-SUMO protease was achieved through a second IMAC, and the albLIPS-2 samples were collected in the flow-through fraction. Finally, the samples were concentrated using Vivaspin Turbo 15 filters (Sartorius, MWCO 10 kDa or 3 kDa) and injected into a Superdex 75 10/300 GL column (Cytiva) equilibrated in 25 mM HEPES/NaOH, 100 mM NaCl, pH 8.0, yielding a single peak.

In the case of Cp19 and Cp19ΔC, during the second IMAC step the protein co-eluted with the cleaved His-SUMO tag. Therefore, prior to size-exclusion chromatography, the proteins were further purified using a ion exchange step. NaCl concentration from the fractions from the second IMAC was lowered using a desalting column (HiPrep 26/10 Desalting, Cytiva) to 50 mM (25 mM HEPES/NaOH, 50 mM NaCl, pH 8.0). A Capto Q anion exchange column (Cytiva), pre-equilibrated with the anion exchange buffer (25 mM HEPES/NaOH, 50 mM NaCl, pH 8.0), was loaded with the protein sample and purification was performed by applying a 1 hour gradient from 50 mM to 500 mM NaCl at pH 8.0. Cp19 elution occurred at 110 mM NaCl.

Protein quality was assessed throughout the purification using reducing and non-reducing SDS-PAGE analysis. Evaluation of protein concentration was carried out by determining the absorbance at 280 nm using 0.82 as extinction coefficient for albLIPS-2 and 1.7 for Cp19, respectively; these values were calculated according to the Expasy ProtParam tool.[67] Purified proteins were concentrated to 18 mg mL^{-1} and stored at -80°C until usage.

Laser scanning confocal microscopy

To visualize any modification of the labrum structure after stimulation with albLIPS-2 protein, mature female mosquitoes were processed as described for the immunofluorescence assay. After removal of the antennae and of the labium, heads were incubated with albLIPS-2 protein (1 mg/mL) or with the protein buffer as control. Subsequently, each sample was mounted on a microscope slice and visualized under the Olympus LEXT OLS4100 3D Measuring Laser Microscope (50X). Images were analyzed using the Olympus OLS400 3.1.9 software. The data used to reconstruct the profiles of the labrum surface at intervals of 10 μm starting from its tip were exported in an Excel file. For each height profile, the lateral resolution of the profile is 125 nm while the height resolution is 30 nm.

In the case of natural exposition to saliva (either controls or dsRNA injected), mosquitoes were let to salivate on a membrane covering a bottle containing warm water. Mosquitoes that were actively probing on the membrane were collected by mouth aspirator and immediately placed in dry ice. The samples were processed as described before (without further incubation in protein mixtures).

Generation of LIPS-2 mutants

To confirm the site of interaction between LIPS-2 and Cp19 proteins, R38S mutant of LIPS-2 was generated. LIPS-2 template was amplified using the following oligonucleotide primers: GFP-LIPS-2fw coupled with R38S_LIPS-2rv (R38Sa) and GFP-LIPS-2rv coupled with R38S_LIPS-2fw (R38Sb). The reaction mixture and the thermal cycling conditions were those used for the screening of the YTH assay between Cp19 and LIPS-2 mutants. R38Sa and R38Sb PCR products were incubated with linearized pET28b vector and NEBuilder HiFi DNA Assembly (NEB) for 1 hour at 50 °C. Transformation of SCCs was carried out as described above. Transformants were selected on LB agar plates supplemented with Kan 50 μg/mL. Plasmid DNA was isolated using standard methods and sequenced using T7 and T7term standard primers. Protein was expressed and purified as previously described.

Control mutant was obtained by coupling GFP-LIPS-2fw with S151AR152Srv and GFP-LIPS-2rv with S151AR152Sfw, and applying the same protocol described above.

Protein unfolding resistance measurements

Initial thermal-shift assays (TSA) unambiguously indicated a strong propensity of albLIPS-2 to interact with the unfolding sensor SYPRO orange, limiting application of conventional Thermofluor methods.[86] We therefore tailored TSA using the molecular rotor 9-(2,2-Dicyanovinyl)julolidine (DCVJ).[87] 20 μL of mixture was prepared in a 48-well plate with 2 mg/ml protein and 10 μM dye final concentrations. Measurements were performed using a MiniOpticon real-time PCR detection system (Bio-Rad) using the SYBR Green filters. Unfolding curves were generated using a temperature gradient from 25 to 95 °C, with a ramp of 0.5 °C and 10 s of delay between readings of the fluorescence. Results were comparable with those obtained with label-free differential scanning fluorimetry (DSF) experiments, carried out using 5 μL of 4 mg mL^{-1} protein in a Tycho NT.6 instrument (Nanotemper).

Circular Dichroism (CD)

CD measurements were performed with a Jasco J-700 spectropolarimeter (Jasco-Europe, Cremella, Italy) using a 1 mm path cell at 25 °C in Buffer A. Scans were conducted between 200 and 250 nm at a speed of 20 nm/min. The protein concentration was 1 mg mL^{-1}. The α-helical and β-sheet content was calculated with K2D3 software.[68]

Please cite this article in press as: Arnoldi et al., A salivary factor binds a cuticular protein and modulates biting by inducing morphological changes in the mosquito labrum, Current Biology (2022), https://doi.org/10.1016/j.cub.2022.06.049

SEC-SAXS

Size exclusion chromatography coupled to small angle X-ray scattering (SEC-SAXS) data were collected at the ESRF BM29 beamline using a sec^{-1} frame rate on Pilatus 1 M detector. Size exclusion chromatography coupled to SAXS (SEC-SAXS) experiments were carried out using Nexera High Pressure Liquid/Chromatography (HPLC; Shimadzu). 50 μL of albLIPS-2 concentrated at 10 mg mL^{-1} were injected into a Superdex 75 3.2/300 PC (GE Healthcare), pre-equilibrated with 25 mM HEPES/NaOH, 100 mM NaCl, pH 8.0. Data were analyzed using CHROMIXS[69] and ATSAS.[70] A summary of data processing results is shown in Table S2.

X-ray data collection and processing

Crystallization experiments were initially carried using the sitting-drop vapor diffusion method using robotic nanoliter dispensing (Oryx 8, Douglas Instruments) of purified albLIPS-2 at 18 mg mL^{-1} concentration with commercial crystallization screens. Initial crystal hits underwent manual optimization using the sitting drop method, yielding crystals of appropriate size for X-ray diffraction experiments in reservoirs composed of 1 M $(NH_4)_2SO_4$, 1 M Li_2SO_4, 0.1 M KNO_3. Crystals were cryo-protected using the reservoir supplemented with 20% glycerol, collected using MicroMounts Loops (Mitegen) and flash-cooled liquid nitrogen. X-ray diffraction data were collected using the automated pipeline available at the MASSIF-1 (ID30A-1) beamline of the European Synchrotron Radiation Facility, Grenoble, France.[88] Data were indexed and integrated using *XDS*[71] and scaled using *Aimless*.[72] Data collection statistics are summarized in Table S3.

Structure determination and refinement

The crystal structure of albLIPS-2 was determined using single wavelength anomalous dispersion (SAD) on Selenomethionine-labelled (SeMet) protein crystals. Data were collected at the ESRF ID23-EH1 beamline (Table S3). Using the HKL2MAP pipeline,[73] SeMet atom coordinates were identified and refined with SHELXC/D,[74] and experimental phasing and density modification was carried out in SHELXE,[74] yielding a clearly interpretable electron density map and a nearly complete polyalanine model. Model building was then performed automatically using ARP/wARP.[75] Iterations of automatic and manual refinements using PHENIX[76] and COOT[77] allowed to obtain the final 3D model. Structural figures were generated using PyMol.[83]

Evaluation of LIPS-mosquito interactions

To visualize the induction of the probing movements, labium, legs and wings were removed from mosquitoes shortly (2-3 min) anesthetized on ice, and the stylet was inserted in a drop of purified albLIPS-2 protein or BSA as control (1 mg mL^{-1} in 25 mM HEPES/NaOH, 100 mM NaCl, pH 8.0) for 30 seconds. The movements were observed under an inverted microscope. Differences between the two groups were tested using χ^2 test adapted to contingency tables.

To visualize the interaction between mosquito proboscis and GFP-albLIPS2 protein, mature female mosquitoes (> 6 days old) were cold-anesthetized, the head separated from the rest of the body and the labium was carefully removed using a pair of fine forceps. The stylet was inserted in a drop of protein solution at 1 mg mL^{-1} for 30 seconds, washed extensively for one minute in a drop of PBS. Stylets were then immediately visualized under an epifluorescence Zeiss Axioplan microscope and images were captured using an Olympus DP70 digital camera.

GFP was used as control.

To test whether LIPS-2 might interact with a protein receptor, legs and wings were removed from anesthetized mosquitoes and the proboscis was inserted in a tip containing 2 μL of a trypsin solution (1 mg mL^{-1} in PBS). PBS without trypsin was used as control. After 1 hr at room temperature, the labium was removed and washed with three passages in PBST. Mosquitoes were then treated as previously described. Differences between the groups were tested using χ^2 test adapted to contingency tables and p values were FDR corrected to avoid statistical type I error for multiple testing.

To test the induction of feeding, mosquitoes were cold anesthetized, the labium, legs and wings removed, and the stylet inserted in a drop of GFP-albLIPS-2 or of GFP as control (1 mg mL^{-1} in PBS). Soon after, the mosquitoes were visualized under an epifluorescence Olympus stereomicroscope and images were captured using an Olympus DP70 digital camera.

MST analysis of protein-protein interaction

LIPS-2:Cp19 *in vitro* binding validation and quantification were performed by using Microscale Thermophoresis (MST) technique on a Monolith NT.115 instrument (Nano Temper Technologies, Germany). To set up the experiments, we used recombinantly expressed and purified proteins GFP-albLIPS-2, GFP-albLIPS-2ΔHTH, GFP-albLIPS-2(R38S), GFP-albLIPS-2(S151A; R152S), and Cp19 as full-length protein (Cp19) or Cp19 lacking the C-terminal region (Cp19ΔC). The experiments were performed with standard MST capillaries screened with 100% MST "LED blue power" (excitation 460-480 nm, emission 515-530 nm), to optimally excite the GFP-albLIPS-2 used as target.

All tests were carried out with 20 nM GFP-albLIPS-2 and GFP-control protein, 110 μM Cp19, 62.5 μM Cp19ΔC in the assay buffer (25 mM HEPES/NaOH, 100 mM NaCl, 0.05% Tween-20, pH 8.0).

MST measurements were performed through the MO.Control software (v1.6), following the manual guide provided by the NanoTemper. Analysis were carried out through the MST analysis software MO.Affinity (v2.2).

To extract dose-response curves, results from MST raw traces from binding affinity tests were analyzed for the normalized fluorescence intensity (Fnorm) at 2.5 seconds, and Kds were obtained fitting the data for the "Kd Model".

To test the possible role of Cp19 C-terminal sequence in the interaction with LIPS-2, an *in vitro* synthetized C-terminal Cp19 polypeptide (Cp19-C; ChinaPeptides) was used at 120 μM, in same assay buffer (25 mM HEPES/NaOH, 100 mM NaCl, 0.05% Tween-20, pH 8.0), a setting also exploited for the in vitro reconstitution of the binding experiment (20 nM GFP-albLIPS-2, 120 μM Cp19-C and 60 μM Cp19ΔC).

QUANTIFICATION AND STATISTICAL ANALYSIS

- For all the analysis $\alpha = 0.05$ if not differently specified.
- Distance-based ANOVA of fuzzy maps of 2D gels has been performed using R.
- Data about mosquito behavior or analysis of morphological and molecular traits (e.g. probing and feeding time, ridges' depth of the labrum and expression of LIPS-2 and Cp19) have been performed in Prism GraphPad software.
- All the details about the numerosity of the samples and the applied analysis are reported in the dedicated section of the text or in the figures and figure legends.
- SEC-SAXS and protein crystal X-ray diffraction data have been analyzed with dedicated software as reported in the text and the results are reported in Tables S2 and S3.